
Recovery of hydrothermal vent communities in response to an induced disturbance at the Lucky Strike vent field (Mid-Atlantic Ridge)

Marticorena Julien ^{1,*}, Matabos Marjolaine ¹, Ramirez-Llodra E. ^{2,3}, Cathalot Cecile ⁴, Laes Agathe ⁵, Leroux Romain ⁶, Hourdez S. ⁷, Donval Jean-Pierre ⁴, Sarrazin Jozee ¹

¹ Ifremer, REM/EEP, F 29280 Plouzané, France

² Norwegian Institute for Water Research, Gaustadalleen 21, 0349 Oslo, Norway

³ REV Ocean, Oksenøyveien 10, 1366 Lysaker, Norway

⁴ Ifremer, REM/GM/LCG, F-29280 Plouzané, France

⁵ Ifremer, REM/RDT/LDCM, F-29280 Plouzané, France

⁶ Research Centre for Watershed-Aquatic Ecosystem Interactions, Université du Québec à Trois-Rivières, Trois-Rivières, QC G9A 5H7, Canada

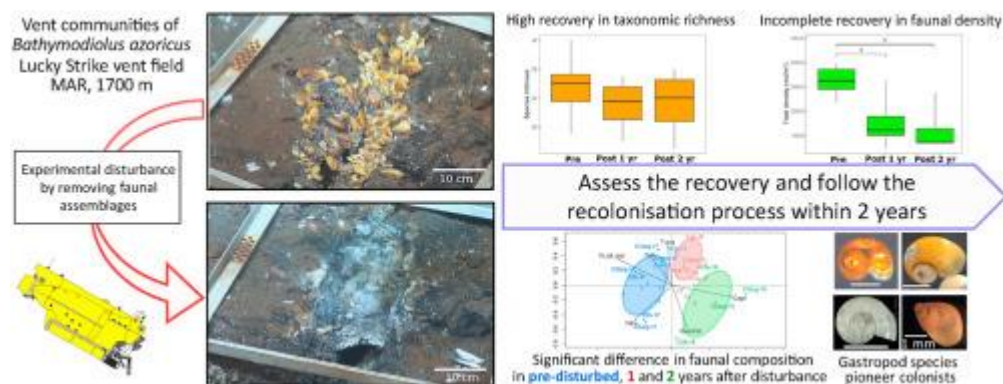
⁷ Observatoire Océanologique de Banyuls-sur-Mer, UMR 8222 CNRS-SU, 1 avenue Pierre Fabre, 66650, Banyuls-sur-Mer, France

* Corresponding author : Julien Marticorena, email address : julienmarticorena@gmail.fr

Abstract :

So far, the natural recovery of vent communities at large scales has only been evaluated at fast spreading centres, by monitoring faunal recolonisation after volcanic eruptions. However, at slow spreading ridges, opportunities to observe natural disturbances are rare, the overall hydrothermal system being more stable. In this study, we implemented a novel experimental approach by inducing a small-scale disturbance to assess the recovery potential of vent communities along the slow-spreading northern Mid-Atlantic Ridge (nMAR). We followed the recovery patterns of thirteen *Bathymodiolus azoricus* mussel assemblages colonising an active vent edifice at the Lucky Strike vent field, in relation to environmental conditions and assessed the role of biotic interactions in recolonisation dynamics. Within 2 years after the disturbance, almost all taxonomic richness had recovered, with the exception of a few low occurrence species. However, we observed only a partial recovery of faunal densities and a major change in faunal composition characterised by an increase in abundance of gastropod species, which are hypothesised to be the pioneer colonists of these habitats. Although not significant, our results suggest a potential role of mobile predators in early-colonisation stages. A model of post-disturbance succession for nMAR vent communities from habitat opening to climax assemblages is proposed, also highlighting numerous knowledge gaps. This type of experimental approach, combined with dispersal and connectivity analyses, will contribute to fully assess the resilience of active vent communities after a major disturbance, especially along slow spreading centres targeted for seafloor massive sulphide extraction.

Graphical abstract



Highlights

► Novel experimental approach by inducing small-scale disturbance to assess the recovery of vent communities. ► Full recovery of faunal taxonomic richness within 2 years after the disturbance ► Incomplete recovery of faunal densities and enhancement of species evenness in post-disturbance communities ► Gastropod species appears to be the pioneer colonists of active vent assemblages ► There are differences in the recovery rate of active vent in comparison to peripheral area and inactive structure.

Keywords : Hydrothermal vent, *Bathymodiolus azoricus*, Disturbance, Colonisation, Recovery, Deep-sea mining, Ecological succession, Benthic ecology, Mid-Atlantic Ridge

45 1. Introduction

46

47 Deep-sea hydrothermal vents are mainly distributed along mid-ocean ridges and
48 back-arc basins. Vent communities are considered as productivity hotspots with a high level
49 of endemic fauna (Tunnidiffe, 1991) that thrives mainly on chemoautotrophic primary
50 production (Childress and Fisher, 1992). Faunal assemblages are often dominated by
51 symbiotic foundation species such as siboglinid tubeworms, mytilid mussels, large provannid
52 gastropods or alvinocaridid shrimps, which promote local diversity by providing 3D
53 structures and enhancing habitat heterogeneity (Dreyer et al., 2005; Govenar and Fisher,
54 2007). At the edifice scale, faunal distribution consists in a mosaic of assemblages mainly
55 influenced by environmental conditions and patchiness of fluid emissions (Sarrazin et al.,
56 1997; Sarrazin and Juniper, 1999; Luther et al., 2001; Gollner et al., 2010; Marsh et al., 2012;
57 Husson et al. 2017). Indeed, species colonise the mixing gradient depending on their
58 physiological tolerance to environmental conditions, nutritional requirements and biotic
59 interactions (e.g. predation, facilitation; Levesque et al. 2003, Mullineaux et al. 2003, Sancho
60 et al. 2005). Biotic interactions were suggested to prevail in high diffuse-flow areas where
61 the resources are not limited, while facilitation will predominate in habitats with lower fluid
62 input (Mullineaux et al. 2003). As observed in coastal hard substrate communities, mosaics
63 are highly dynamic and patches size and boundaries amongst the patched may change
64 through time (Connell and Keough, 1985). At large spatial scale, the patchiness of vent
65 habitat results in a network of metacommunities and population connectivity is insured by
66 dispersal of planktonic larvae (Mullineaux et al., 2018).

67 Hydrothermal vents are naturally subject to stochastic major disturbance such as
68 volcanic eruptions that may eradicate faunal assemblages at the vent-field scale. On the
69 other hand, since the first discovery of hydrothermal vents and associated seafloor massive
70 sulphide (SMS) deposits, more than 40 years ago, the interest of mining companies for
71 commercial exploitation of their high metal content has been increasing (Corliss et al., 1979;
72 Spiess et al., 1980; Van Dover, 2011). These industrial activity has not yet started, but it is
73 predicted that they may induce different levels of impacts (Boschen et al., 2013; Cuvelier et
74 al., 2018; Orcutt et al., 2020), including physical destruction of habitats and the complete
75 eradication of their faunal communities within the mining site (Van Dover 2007). The
76 creation of a sediment plume may also affect different biological processes, such as

77 reproduction, dispersal, mobility and feeding strategies at larger scale (Van Dover, 2010;
78 Boschen et al., 2013; Gollner et al., 2017; Suzuki et al., 2018; Washburn et al., 2019).
79 However, there are still many uncertainties about community resilience, and the time-scale
80 needed for a possible recovery of the impacted ecosystems (Cuvelier et al., 2018).

81 Disturbance in mosaic habitats such as active vents may play an important role in
82 initiating, maintaining or enlarging patches within established assemblages (Sousa 1985;
83 Denny 1987). The fundamental question of recolonisation and recovery of vent assemblages
84 after a disturbance can be studied in a metacommunity framework, using a patch dynamics
85 approach in which the colonisation and persistence of impacted area is highly dependent on
86 dispersal across vent fields and local disturbance regimes (Leibold et al., 2004; Mullineaux et
87 al., 2018). At local scale, the settlement of post-larvae is influenced by environmental
88 conditions and habitat suitability and recolonisation dynamics are also dependent on biotic
89 interactions that may induce facilitation or competitive exclusion (Mullineaux et al., 2003;
90 Sancho et al., 2005). Understanding processes acting at small scales are paramount in
91 evaluating mechanisms controlling successional dynamics after recolonisation by species
92 from afar.

93 At active vents, the few examples of recovery are based on studies linked to large-
94 scale natural disturbances caused by volcanic and tectonic activities (Butterfield et al., 1997;
95 Tunnicliffe et al., 1997; Shank et al., 1998; Marcus et al., 2009; Gollner et al., 2015a). The
96 frequency of such disturbances is highly variable among vent systems, depending on their
97 geological settings. At fast-spreading ridges, where vent sites are separated by a few
98 kilometers, volcanic eruptions occurs with time intervals of a decade (Tolstoy et al. 2006)
99 and macrofaunal communities show a fairly good recovery of diversity and densities within
100 few years following the various eruptions (Tunnicliffe et al. 1997; Shank et al. 1998; Marcus
101 et al. 2009; Gollner et al. 2015a, 2017, 2020). However, differences in the sampling
102 methodology between these studies (e.g. some used visual surveys while others sampled
103 faunal assemblages) and the faunal compartment considered lead to differences in the
104 estimation of recovery rates. Moreover, little information about the pre-disturbed baseline
105 communities was available, making the comparison with post-disturbance communities
106 difficult. Differences in community composition after re-colonisation were also observed
107 (Mullineaux et al., 2020, 2012) and the prolonged monitoring of diversity showed that
108 community composition was still changing ten years after the disturbance, suggesting that

109 the disturbed assemblages did not reach a climax stage during this time period (Mullineaux
110 et al., 2020). Conversely, at slow spreading ridges, vent sites are separated by hundreds of
111 kilometers (Beaulieu et al., 2015) and opportunities to observe natural disturbances are rare.
112 Therefore, assessing the recovery ability of communities requires the use of alternative
113 indirect approaches. One way is to use population connectivity data to estimate the
114 recolonisation potential of key species, and thus infer vent community recovery rates (Baco
115 et al., 2016; Breusing et al., 2016) as it was done by Suzuki et al. (2018). Their dispersal
116 network analysis on species from 131 vent fields of the western Pacific Ocean estimated that
117 a full recovery to original communities would take from 6 to 130 years. The slow recovery
118 rate estimated in comparison to fast-spreading centers may notably be due in part to
119 differences in topography that may reduce horizontal dispersal and connectivity (Mullineaux
120 et al. 2018). However, this approach based on dispersal ability does not take into account
121 the local factors influencing faunal establishment and many uncertainties remain regarding
122 the role of biotic and abiotic conditions in recolonisation dynamics and ecological succession
123 once the larvae reach the disturbed area.

124 In the present study, we provide an early evaluation of the recovery potential of
125 active vent communities to a small-scale ($< 1 \text{ m}^2$) disturbance experiment initiated in 2017
126 on the Lucky Strike (LS) vent field, northern Mid-Atlantic Ridge (nMAR). After removing the
127 fauna, we followed during 2 years the recolonisation dynamics of *Bathymodiolus azoricus*
128 mussel assemblages and their habitats on a series of experimental quadrats. This
129 experimental setting allowed us to describe the pre-disturbed structure of vent communities
130 on the Montségur edifice (LS) and to monitor the recolonisation of benthic communities
131 after the disturbance. The main objective of this work is to identify the role of biotic and
132 abiotic conditions on recolonisation dynamics at the edifice scale, through the use of cages
133 and measurements of environmental conditions. We expected that microbial communities
134 would first colonise the bare substratum, followed by grazers (including several species of
135 gastropods) that may feed on microbial mats. The engineer species *B. azoricus* would take
136 more time to fully occupy the space, its presence facilitating the establishment of associated
137 taxa and contributing to increasing diversity. We anticipated that mobile predators (e.g.
138 shrimps, crabs or fishes) would play a major role in patch colonisation, influencing the first
139 step of recovery. Although the scale and target of this experiment strongly differ from large-

140 scale disturbance, our results provide fundamental knowledge on recolonisation patterns of
141 active hydrothermal vent habitats at the edifice scale.

142 2. Material and methods

143

144 2.1. Study site

145 The Lucky Strike (LS) vent field is a basalt-hosted vent field situated close to the Azores Triple
146 Junction on the northern part of the Mid Atlantic Ridge (MAR) (Langmuir et al., 1997) (Fig.
147 1A). LS contains over twenty active hydrothermal edifices distributed around a circular
148 fossilised lava lake at an average depth of 1700 m (Ondreas et al., 2009). Montségur is a
149 small active sulphide edifice that extends over a surface of 24 m x 16 m. It is located on a flat
150 hydrothermal slab at the south-east of LS (Fig. 1B). At least seven black smokers have been
151 identified on the edifice, in addition to the extensive diffuse low-temperature discharges
152 through cracks at its base and on its flanks (Barreyre et al., 2014). Montségur is covered by
153 dense mussel assemblages of the engineer species *Bathymodiolus azoricus*. Vent faunal
154 communities inhabiting diffuse flow areas on and around the edifice are characterised by
155 high-density populations of gastropods (*Protolira valvatoides*, *Lepetodrilus atlanticus*,
156 *Pseudorimula midatlantica*), polychaetes (*Branchiopolynoe seepensis*, *Amphisamytha lutzi*)
157 and shrimps (*Mirocaris fortunata*) (Sarrazin et al. 2020).

158 2.2. Experimental setup

159 In July 2017, an experimental setup was deployed during the Momarsat cruise on board the
160 R/V "Pourquoi pas ?" using the Remotely Operated Vehicle (ROV) Victor6000. Thirteen
161 stainless steel quadrats (50 x 50 cm), equipped with pyramidal structures on top, were
162 installed over *Bathymodiolus azoricus* assemblages (Fig. 2), on the steep walls of the
163 Montségur edifice or in cracks at its base (Fig. 1C), to account for spatial variability of vent
164 assemblages. Eight of them, named "experimental quadrats", were devoted to the study of
165 recolonisation processes following faunal clearance after 1 (C1) and 2 (C2) years (August
166 2018 and June 2019 respectively). Replicate samples for each year were denoted as "a" or
167 "b" (Fig. 1C). In addition to the experimental quadrats, five "reference" quadrats (R) were
168 deployed and sampled in 2017 (R0a, R0b), 2018 (R1) and 2019 (R2, R2cg) to characterise the
169 natural dynamics of faunal communities on Montségur throughout the experiment. The role
170 of large mobile predators (crabs, shrimp or fish) on local recolonisation was examined by

171 covering some of the pyramidal structures with a 1 cm plastic mesh. These specific quadrats
172 were denoted as “cg” for caged (Fig. 2C). This experimental design is summarised in Figure 3.

173

174 2.3. Environmental characterisation

175 Temperature and key chemical parameters were assessed from in situ measurements on all
176 quadrats before and after faunal sampling and this, for each year of the study (2017 to
177 2019). Our objectives were to identify the spatial and temporal variability of these factors
178 and evaluate their role in the recolonisation processes. The in situ chemical analysers
179 CHEMINI (Vuillemin et al., 2009) were used on three replicate points in each quadrat to
180 measure dissolved concentration of total sulphides [TdS : $H_2S+HS^-+S_2$] and total dissolved
181 iron [TdFe : Fe (II)]. To complete the chemical characterisation, water samples were
182 collected with the PEPITO water sampler at each quadrat prior to faunal sampling (Sarradin
183 et al., 2009). Oxygen concentrations were measured using an Aanderaa optode probe
184 (Tengberg et al. 2006) connected to the outlet of the PEPITO sampler. Methane [CH_4], was
185 analysed back in the laboratory by GC-FID and HID (Donval et al. 2008). In addition to this
186 one-time yearly characterisation, temperature was monitored every 2 hours over the
187 deployment period using two iButtonsTM probes attached to each quadrat and deployed
188 directly on the mussel assemblages with a measurement resolution of 0.5 °C.

189

190 2.4. Faunal sampling and identification

191 During the Momarsat 2017 cruise, eight experimental quadrats -noted “C”- were cleared of
192 their fauna using both the suction sampler and the claw of the ROV Victor6000 mechanical
193 arm (Fig. 2A, 2B). The same year, R0a and R0b reference quadrats were also sampled,
194 leading to a total of 10 quadrats used to describe the pre-disturbed vent community of
195 Montségur (Fig. 3). During Momarsat 2018, the four experimental quadrats dedicated to the
196 “one-year after disturbance recolonisation study” -noted “C1”- and reference quadrat R1
197 were sampled (5 quadrats in total; Fig. 3). During the Momarsat 2019 cruise, the four
198 experimental quadrats dedicated to the “two-year after disturbance recolonisation study”
199 noted “C2”-and reference quadrats R2 and R2-cg were sampled (6 quadrats, Fig. 3). The
200 surface area of each quadrat was filmed before and after faunal sampling with the ROV high
201 definition cameras to estimate the sampled surfaces using imagery analysis (Fig. 2A, 2B). A

202 target with 7 mm checkerboard squares was fixed on each quadrat, providing scaling in the
203 field of view (Fig. 2B).

204 In this study, fauna will include macrofauna and any meiofauna taxa larger than 250 μm
205 (nematodes, copepods and ostracods). We also include species often considered as
206 megafauna (shrimp, mussels) recovered within the quadrats. The faunal samples were
207 preserved in 96% ethanol. All individuals collected were identified to the lowest possible
208 taxonomic level under a stereomicroscope and counted.

209 2.5. Population size structure

210 Size-frequency distributions of the six most dominant species were analysed for each sample
211 of the Montségur edifice. Each individual was measured, using different measurements
212 depending on the species (see details in Table S1). The biggest individuals were measured
213 using a caliper while small individuals were measured on screen to the nearest 0.001 mm,
214 using the Leica Application Suite software. Measurement error was calculated as the
215 maximum difference among 10 measurements of the same individual on 10 specimens
216 comprising a range of all sizes for each species (Table S1). For each assemblage sampled,
217 length-frequency distribution was plotted for the six species. Size class intervals were chosen
218 according to three criteria: i) most size-classes must have at least five individuals; ii) the
219 number of adjacent empty classes must be minimised; and iii) the interval has to be greater
220 than the measurement error (see Jollivet et al. 2000). Size-frequency distributions were
221 compared to a normal distribution using a one-sample Kolmogorov-Smirnov test and
222 differences between the pre-disturbed and post-disturbance communities were identified
223 using a pairwise Kolmogorov-Smirnov test. Non-parametric Wilcoxon-Mann-Whitney tests
224 were performed to identify differences in mean individual size between the pre-disturbed
225 community and the novel one, after the recolonisation processes in each location.

226 2.6. Data analyses

227 All analyses were computed in R environment (R Core Team, 2018). Species rarefaction
228 curves were computed for each sample, habitat and year to verify the robustness of the
229 sampling effort and characterise the overall diversity. Local diversity was estimated for each
230 assemblage by computing α -diversity indices such as species richness (S), Shannon entropy
231 (H) and the Pielou's evenness index (J') using the vegan package in R (Oksanen et al., 2019).

232 Contingency tables were weighted by the sampling surface for each quadrat for comparison
233 purposes. The resulting density data were used for all subsequent analyses.

234 **Environmental conditions** – The temperatures measured by the iButtonsTM probes were
235 used to characterise each assemblage/quadrat. Four temperature parameters were
236 compiled, including the average (T.avg), minimum (T.min), maximum (T.max) and standard
237 deviation (T.sd). In addition, average concentrations of oxygen (O₂), methane (CH₄), total
238 dissolved iron (TdFe) and sulphides (TdS) as well as standard deviations of TdFe and TdS
239 were used to characterise the spatial variability of abiotic factors among the different
240 Montségur quadrats. A principal component analysis (PCA) was built with all environmental
241 variables (packages FactoMineR and factoextra - Kassambara and Mundt 2019) to identify
242 patterns in environmental conditions among quadrats and determine which variables
243 accounted for most of the observed variance. Finally, Whittaker-Robinson periodograms,
244 programmed in the R package adespatial (Dray et al., 2020) were used to screen for
245 significant periodicities in temperature time series.

246 **Community structure** – A canonical redundancy analysis (RDA) was performed on Hellinger-
247 transformed densities and environmental variables retained by a forward selection (vegan
248 package - Oksanen et al. 2019) to evaluate the spatial variability of community composition
249 in relation to abiotic factors in the baseline communities on the Montségur edifice. This
250 allows us to evaluate the representativeness of baseline communities in Montségur in
251 comparison with faunal assemblages already described on other active edifices of the Lucky
252 Strike vent field.

253 **Recovery patterns** – Faunal recovery patterns were assessed from experimental quadrats.
254 Differences in faunal composition among quadrats along the recolonisation processes were
255 tested using a non-parametric analysis of similarity (ANOSIM; Anderson 2001). The ANOSIM
256 R value is based on differences in average ranking of dissimilarity indices (i.e. Bray-Curtis
257 dissimilarity matrix) between and within the different predefined groups (here each
258 recovery stage, i.e.: pre-disturbed state, one year and two years after disturbance). A RDA
259 on Hellinger-transformed densities data was also used to identify the role of environmental
260 conditions and biotic interactions (i.e. by testing the cage effect) on the structure of
261 macrofaunal assemblages during the recolonisation processes. A variable named “quadrat”
262 was used to evaluate the independence of the samples from the same quadrat over the

263 years in the explanatory environmental matrix. Moreover, to test for the effect of time after
264 disturbance, we coded a quantitative variable named “Yr-aft-dist” (i.e. year after
265 disturbance). In this framework, pre-disturbed reference samples were considered as
266 baseline communities at an equilibrium state and thus were coded with a value greater than
267 2 years. As the age of the natural community is unknown, analyses were run with different
268 values [3 years, 10 years and 100 years] but they all yielded to similar results. Based on
269 previous studies about the temporal stability of these communities (more than 14 years on
270 Eiffel Tower, Cuvelier et al. 2011b) and data about recovery time in other vent system after a
271 major disturbance (4-5 years, Gollner et al. 2017), we considered 10 years as a good
272 compromise to be used for the analysis.

273

274 3. Results

275 3.1. Environmental conditions

276 Mean temperature among the different quadrats of Montségur varied between 5.2 °C and
277 9.5 °C (Table 1). R1 and C2a exhibited the highest maximum temperatures (with maximum of
278 16.1 °C and 22.1 °C respectively), but also higher concentrations in TdFe and CH₄ associated
279 with a more acidic pH (Table 1, Fig. S1).

280 The two temperature probes separated by ~ 10 cm deployed on each quadrat were used to
281 characterise the spatial variability of abiotic conditions at fine scales. While homogeneous
282 temperatures are observed within some quadrats (e.g. C1a, C1bcg, C2b, C2bcg), others
283 showed a high variability of temperatures in the narrow spatial gradient (few centimetres,
284 e.g. C1b, C2acg); (Fig. S2).

285 Notable differences in temperature on single quadrats between the two years were
286 observed. C1b, C1acg and C2a quadrats showed a sharp decrease in mean and variability of
287 temperatures at different times during the first year of deployment (Fig. S2). Periodogram
288 analyses carried out on temperature time series revealed significant periods of 12 h for most
289 quadrats. In addition, significant periods of 24 h were also identified on all quadrats except
290 C1acg. Additional periodic signals, possibly harmonics related to the tidal signal, with periods
291 of 36 h and 48 h, were also revealed for C1a, C1acg and C1bcg.

292 3.2. Pre-disturbed communities

293 The rarefaction curves built for each pre-disturbed sample of Montségur (Fig. S3) nearly
294 reached an asymptote showing that the sampling effort was sufficient to capture the overall
295 taxonomic diversity of macrofaunal benthic communities of active vent habitats. In total, 43
296 taxa were identified among a total of 34 158 individuals in the different samples. Most
297 assemblages were characterised by a taxonomic richness varying between 19 and 28 (Table
298 S2). The C1a sample, which is the only quadrat located on the west side of the edifice,
299 displayed the highest taxonomic richness with the occurrence of 32 taxa, while R2 showed
300 only 12 taxa among 133 identified specimens (Fig. 4; Table S2). Macrofaunal communities
301 were dominated by six taxa: the engineer species *Bathymodiolus azoricus* and its commensal
302 worm *Branchipolynoe seepensis*, the polychaete *Amphisamytha lutzi* and three species of
303 gastropods *Lepetodrilus atlanticus*, *Protolira valvatoides* and *Pseudorimula midatlantica*.
304 Together, they accounted for $68.3 \pm 15.7\%$ of the total abundance. The nematode
305 *Oncholaimus dyvae* and copepod *Aphotopontius* sp., which are typical meiofaunal species,
306 were also abundant in the $> 250 \mu\text{m}$ fraction of most samples. In the pre-disturbed
307 community, $\sim 74\%$ of taxa (e.g. 29 taxa over 43) showed low occurrence and abundance (i.e.
308 below 1% frequency) in the different samples (Table S3).

309 A RDA has been performed to identify the role of environmental conditions on faunal
310 distribution and verify the temporal stability of baseline communities. The RDA model
311 performed on Hellinger-transformed species densities accounted for 49.6% (adjusted R^2 :
312 25.1%, $p = 0.008$) of the total inertia in macrofaunal species assemblage structure (Fig. 5).
313 The overall RDA model was significant (p -value = 0.004) and only the first axis was significant
314 ($p = 0.05$), accounting for 20% of the variation in community structure. Maximum
315 temperature (T.max) and total dissolved sulphide concentrations (TdS) were the significant
316 environmental factors influencing macrofaunal composition ($p = 0.009$ and 0.021 ,
317 respectively). The years at which the samples were collected did not explain the differences
318 between quadrats. R2cg sample stood out from the other sampling locations and was
319 characterised by a high relative density of the gastropod *Lurifax vitreus*, contrasting with a
320 low density of *B. azoricus* (Fig. 5). Moreover, the C2acg and R0b samples, characterised by a
321 high density of amphipods (*Luckia striki*), formed a distinct group (Fig. 5). All other samples
322 showed a quite homogeneous faunal composition.

3.3. Recovery patterns of benthic communities

323 3.3. Recovery patterns of benthic communities
324 Recolonisation dynamics of the foundation species – The recovery rate of *Bathymodiolus*
325 *azoricus*, in terms of density, varied between 9.7% and 37.6% on the different quadrats one
326 year after disturbance, and from 1.9% to 33% two years after disturbance (Fig. 6). No
327 significant difference can be noticed between the mean recovery rate after 1 year ($19.8 \pm$
328 13%) and 2 years of recolonisation ($14.4 \pm 13.5\%$) (Student test: $t = 0.59$, $p\text{-value} = 0.58$).
329 However, with the exception of the C2bcg quadrat, the percentage of recovery was slightly
330 higher in the quadrats that were caged during the recolonisation process ($>20\%$) compared
331 to the uncaged quadrats ($<15\%$) (Fig. 6). The size population structure analyses of *B. azoricus*
332 showed individuals ranging from 251 μm to 8.5 cm length within the different assemblages
333 (Fig. 6). The pre-disturbed structure of the population on Montségur showed a polymodal
334 size distribution dominated by a large proportion (i.e. 52% of the overall population) of small
335 individuals below 5 mm in shell-length and a tail of distribution in larger sizes containing
336 several cohorts (Fig. 6). Pairwise Kolmogorov-Smirnov distribution tests showed significant
337 differences in population size structure between the pre-disturbed and post-disturbance
338 communities in all samples ($p\text{-value} < 0.001$), except C2b ($D = 0.10$, $p\text{-value} = 0.13$) (Fig. 6).
339 Furthermore, Wilcoxon-Mann-Whitney tests highlighted that the mean shell length of *B.*
340 *azoricus* was smaller 1 and 2 years after the disturbance compared to that of the pre-
341 disturbed community for all samples except C1a and C2b (Fig. 6). Furthermore, the
342 proportion of juveniles of *B. azoricus* (< 5 mm) in the overall population was higher in
343 assemblages sampled 1 year (67%) and two years (70%) after the disturbance in comparison
344 to pre-disturbed populations (52%) (Table S3).

345 Recolonisation dynamics of active vent communities – The rarefaction curves did not level
346 off for most of the post-disturbance samples on Montségur, but they show similar trends
347 than that of pre-disturbed communities (Fig. S3). The shape of the curves indicate that they
348 should reach a plateau earlier, highlighting a higher evenness in the recovering communities.
349 Species richness (S) is lower (from 1 to 6 less species) in the post-disturbance assemblages
350 compared to the pre-disturbed communities 1 year after the induced disturbance (Fig. 4A,
351 Table S2). On the other hand, two years after, the C2a and C2acg quadrats showed a higher
352 species richness than pre-disturbed quadrats, while C2b and C2bcg exhibited lower values
353 after the disturbance (Fig. 4A, Table S2). Overall, species richness was homogeneous
354 between all samples and was not significantly different along the recolonisation process

355 (Kruskal-Wallis test: $P= 1.17$, $p\text{-value} = 0.56$, Fig. 4A). However, macrofaunal densities were
356 significantly lower after 1 year ($15\,768 \pm 12\,487 \text{ ind.m}^{-2}$) and 2 years ($11\,190 \pm 8\,270 \text{ ind.m}^{-2}$)
357 after the disturbance, in comparison to the pre-disturbed community ($34\,402 \pm 7\,590 \text{ ind.m}^{-2}$)
358 ($P= 7.65$, $p\text{-value} = 0.021$ and Post hoc Dunn test: $p\text{-value} < 0.05$, Fig.
359 4A) with a density recovery rate ranging from 15.7% on C1b after 1 year to 79.6% on C2acg 2
360 years after the disturbance (Fig. 6, Table S2). The Shannon index and Pielou's evenness were
361 highly variable across samples in the pre-disturbed communities, but higher 1 year and 2
362 years after the disturbance (Fig. 4C and 4D, Table S2). Overall Pielou's evenness index is
363 significantly higher in post-disturbance communities compared to pre-disturbed
364 communities (Kruskal-Wallis test: $P= 7.34$, $p\text{-value} = 0.026$ and Post hoc Dunn test: $p\text{-value} <$
365 0.05 , Fig. 4D). In the same way, the proportion of low occurrence species is lower in post-
366 disturbance communities (60% after 1 year and 58% after 2 years) than prior to the induced
367 disturbance (74%) (Table S2).

368 The output of the RDA computed on Hellinger-transformed densities of the different species
369 along the recolonisation process showed a significant difference in faunal composition
370 between the pre-disturbed communities and post-disturbance communities at Montségur
371 (Fig. 7). The RDA model explained 42% (Adjusted $R^2 = 20.5\%$) of the total inertia in species
372 assemblage structure ($p\text{-value} = 0.006$). The main driver of this observed difference is time
373 after the induced disturbance ($p\text{-value} = 0.001$), whereas no significant cage effect or
374 dependence between sites were observed ($p\text{-values} = 0.300$ and 0.262 , respectively). The
375 analysis of similarity (ANOSIM) on Bray-Curtis dissimilarity matrix suggests a major change in
376 macrofaunal composition between pre-disturbed communities and those after 1 and 2 years
377 of recolonisation ($R = 0.712$, $p\text{-value} = 0.001$). However, no significant difference in faunal
378 composition was identified between the assemblages collected 1 year and those collected 2
379 years after the disturbance.

380 Some species appeared to play a major role in the observed differences along the
381 recolonisation process (Fig. 8). Indeed, a decrease in the abundance of the typical vent
382 species (*Bathymodiolus azoricus*, *Branchipolynoe seepensis*, *Amphisamytha lutzi* and
383 *Lepetodrilus atlanticus*) was observed in the post-disturbance communities, while small
384 gastropod species (i.e. *Lurifax vitreus*, *Protolira valvatoides*, *Laeviphitus desbruyeresi*,
385 *Xylodiscula analoga*) and nematodes (*Oncholaimus dyvae*) showed a significant increase in

386 the post-disturbance communities (Fig. 8, Fig. S4). *Pseudorimula midatlantica* and the
387 copepod *Aphotopontius* sp. displayed higher relative abundances in the first year after the
388 disturbance in comparison to the pre-disturbed community and returned to lower values 2
389 years after the disturbance. As observed for *B. azoricus*, the other dominant species
390 displayed a polymodal structure of size distribution and differences have been identified
391 between the pre-disturbed community and post disturbance state (pairwise Kolmogorov-
392 Smirnov test) (Fig. S4). Furthermore, individuals of *A. lutzi*, *B. seepensis*, *L. lepetodrilus* and *P.*
393 *valvatoides* were overall smaller within the communities after disturbance in comparison to
394 those of the pre-disturbed community in most quadrats (Fig. S4). For *P. midatlantica*, only 1
395 quadrat showed significant differences in population size structure (Fig. S4).

396 4. Discussion

397 In this study, we provide an early evaluation of the recovery of deep-sea benthic
398 communities to a small-scale (<1 m²) disturbance experiment at an active hydrothermal
399 edifice located on the Lucky Strike vent field. The structure of pre-disturbed communities
400 and their recovery patterns were characterised through the analysis of faunal composition,
401 diversity, population size structure in relation to biotic and abiotic factors at the Montségur
402 edifice. This experimental design represents an innovative approach to assess the recovery
403 of vent communities in areas where opportunities to observe natural disturbances are rare.
404 It provides useful insights about local recolonisation drivers at hydrothermal vents, data that
405 can contribute to the elaboration of conservation strategies in the context of potential deep-
406 sea mining activities on seafloor massive sulphides.

407

408 4.1. Habitat characterisation

409 In active vent ecosystems, environmental factors are strongly linked to the output flux and
410 chemistry of hydrothermal fluids and the resulting physico-chemical conditions along the
411 mixing gradient between vent fluids and surrounding sea water. Within the active habitats
412 sampled in this study, mean temperature among *Bathymodiolus azoricus* faunal assemblages
413 varied from 5.2 to 9.5 °C with a maximum of 22.1 °C, which corresponds to the temperature
414 ranges of Eiffel Tower habitats (Husson et al. 2017, Sarrazin et al. 2020). We identified two
415 microhabitats hosting *B. azoricus* assemblages, which have previously been described as cold
416 and warm habitats in Sarrazin et al. (2015). However, while in our study these habitats are

417 colonised by mussels, in the previous study warm habitats were rather reported to be
418 associated with shrimp assemblages. This discrepancy could be related to temperature
419 measurements: in the present study, temperature was measured using iButtonsTM deployed
420 on or within the mussels while most measurements reported previously were conducted
421 using the ROV probe placed a few millimeters above the faunal assemblages (Cuvelier et al.
422 2014a, Husson et al. 2017, Sarrazin et al. 2015, 2020). The rapid mixing of the warm fluids
423 with the above cold seawater can account for these differences. Similar to previous studies,
424 most samples belonging to the cold habitat showed small variability in environmental
425 conditions and were associated with low temperature, low concentrations of iron and
426 sulphides, high pH and high concentrations of dissolved oxygen (Cuvelier et al. 2011a;
427 Sarrazin et al. 2015). However, a few quadrats (R1, C2a and R0b) were characterised by
428 higher temperatures, total dissolved sulphide and iron concentrations as well as lower
429 dissolved oxygen concentrations with acidic pH, which are more representative of warm
430 habitats.

431
432 The continuous bi-hourly monitoring of temperature revealed a high spatial variability in
433 temperature regime (up to 3°C across 10 cm), suggesting the occurrence of multiple
434 microhabitats within a single quadrat. This was supported by high standard deviation values
435 of replicate measurements for sulphides and iron concentrations performed every year. This
436 small-scale temporal variability of temperature can be a result of several processes,
437 including the interplay between sulphide and oxygen biological uptake (Johnson et al.,
438 1988), the formation of diffuse fluids in the subsurface, the chemical reactivity of the mixing
439 zone, the porosity of the substratum in active habitats on the East Pacific Rise (Butterfield et
440 al. 1990; Sarrazin et al. 2002, Le Bris et al. 2006) or tidal oscillations (Barreyre et al. 2014).
441 Our results show significant semi-diurnal and diurnal periods and harmonics, supporting the
442 presence of periodic oscillations related to tidal processes. Tidal modulation of diffused-flow
443 has been reported in many vent systems (Cuvelier et al., 2014b; Sarrazin et al., 2014;
444 Scheirer et al., 2006). These variations are mainly caused by tidally induced currents
445 (Barreyre et al., 2014; Khripounoff et al., 2008) and changes in hydrostatic pressure on the
446 seafloor (Davis and Becker, 1999). This periodicity could be beneficial for symbiotic sessile
447 species that need alternative inputs of reduced compounds and oxygen to ensure

448 chemosynthesis (Scheirer et al. 2006, Mat et al. 2020) but can also influence the behaviour
449 of mobile species (Lelièvre et al., 2017).

450

451 4.2. Pre-disturbed communities and natural variability

452

453 On the active Montségur edifice, all experimental quadrats were visually dominated by
454 medium-sized *B. azoricus* mussels from 5.2 ± 8.8 mm to 24.4 ± 14.3 mm. These sizes are
455 consistent with the mean lengths reported by Comtet and Desbruyères (1998) on different
456 edifices of Lucky Strike (between 5.63 ± 5.67 mm and 49.63 ± 31.41 mm), but smaller than
457 those measured by Sarrazin et al. (2015) on the nearby Eiffel Tower edifice (between $22.7 \pm$
458 18.07 and 74.7 ± 2.57 mm). Indeed, we observed a high proportion (between 52 and 96%) of
459 very small individuals -below 3 mm- in each sample, sizes that correspond to post larval and
460 juvenile stages. The presence of several successive cohorts suggests the occurrence of a
461 massive recruitment event around June, just before sampling. These results are consistent
462 with the lifecycle of *B. azoricus*, with an annual spawning event in January followed by a
463 planktotrophic larval development and the settlement of post-larvae in May-June (Colaço et
464 al., 2006; Comtet and Desbruyères, 1998; Dixon et al., 2006). Furthermore, differences in
465 mean shell length of *B. azoricus* observed among samples on pre-disturbed communities
466 may be due to spatial segregation of sizes related to environmental factors (Sarrazin et al.,
467 2015; Husson et al., 2017) or to biotic interactions (e.g. competition, predation) that may
468 play an important role in recruitment success and survival of post-larvae (Lenihan et al.,
469 2008; Sancho et al., 2005).

470

471 All samples collected at the active Montségur edifice were dominated by the same
472 macrofaunal species (e.g. *B. azoricus*, *B. seepensis*, *A. lutzi*, *P. valvatoïdes* and *L. atlanticus*),
473 which have been previously described as indicator species of cold microhabitats on the Eiffel
474 Tower edifice situated ~ 50 m from Montségur (Sarrazin et al., 2015b). The high similarity
475 between the fauna from the two edifices may be related to their belonging to the same
476 chemistry domain (Chavagnac et al. 2018, Sarrazin et al. 2020). Among the 43 macrofaunal
477 species identified on Montségur, approximately 74% exhibit a low frequency of abundance
478 ($<1\%$). Total densities of organisms in the pre-disturbed communities ranged from 3 330 to
479 $68\ 960\ \text{ind.m}^{-2}$ across the different samples, and is much lower than the values reported by

480 Sarrazin et al. (2020) on the same edifice (between 62 253 and 126 437 ind.m⁻²). In several
481 studies, small mussel assemblages, inhabiting cold microhabitats, harbour higher density and
482 diversity of associated species than large mussel assemblages, found in warmer
483 microhabitats (Cuvelier et al., 2009; Dreyer et al., 2005; Sarrazin et al., 2015). Surprisingly, in
484 this study the highest densities of organisms have been observed in the warmest and more
485 variable habitats. This result may be linked to the differences in the method for assessing
486 temperature as mentioned above. Indeed, temperature values obtained by probes deployed
487 directly on the substratum are expected to be higher than the ones obtained with the ROV
488 probe a few millimeters above faunal assemblages.

489
490 As expected, macrofaunal distribution was significantly influenced by environmental
491 conditions, especially by mean temperature and mean concentrations in total sulphides and
492 methane, in addition to slightly acidic conditions (pH <7.3). However, biotic factors such as
493 competition for space and food resource, but also predation or facilitation, may also play an
494 important role in faunal distribution in diffuse flow habitats (Sarrazin et al. 1997, Sen et al.
495 2013; Gollner et al. 2015b; Husson et al. 2017). On the other hand, faunal composition
496 within reference quadrats did not differ over the three years of the experiment, suggesting a
497 relative stability of the community over time. This supports the observed high stability of
498 mussel communities on the nearby Eiffel Tower edifice, which led to the assumption that *B.*
499 *azoricus* assemblages at Lucky Strike can be considered as a “climax” community (Cuvelier et
500 al., 2011b). The absence of natural changes in faunal assemblages, at the edifice scale,
501 during the experiment allows us to use them as a baseline to test the effect of the induced
502 disturbance on benthic communities.

503

504 4.3. Recolonisation processes and recovery

505

506 In Figure 9, we propose a succession model of nMAR vent communities based on the present
507 experiment at the Lucky Strike vent field and from previous studies conducted after natural
508 disturbances at vents. The first step after the disturbance relies on the release of an
509 ecological niche induced by the removing of faunal assemblages. Then, the stabilisation of
510 environmental conditions, especially of temperature and reduced compounds, would allow
511 chemoautotrophic primary production and proliferation of microbial mats, as observed in

512 studies from vents in the Pacific Ocean (Marcus et al., 2009; Shank et al., 1998; Tunnicliffe et
513 al., 1997). This is followed, within one year, by the arrival of mobile opportunistic species,
514 including shrimps and copepod species. Although not significant, our results suggest that
515 these predator species may slow down the settlement of associated species, resulting in a
516 poor recovery of faunal densities despite a good species richness recovery. Two years after
517 the disturbance, the settlement of several gastropod species grazing on free-living microbial
518 mats have been observed. At this stage, the higher Pielou's evenness compared to baseline
519 communities suggests that biotic interactions are not yet fully effective within assemblages.
520 Gastropods have already been described as main pioneer colonists at 9°N EPR after the 2006
521 volcanic eruption (Mullineaux et al., 2012, 2010). Indeed, despite contrasting reproductive
522 characteristics, some of them are able to maintain an important effective population size
523 and support high abundances, especially through an early maturity and continuous
524 gametogenesis (Marticorena et al., 2020). Thereafter, we hypothesise a later settlement of
525 the foundation species *B. azoricus* due to its seasonal reproduction, which leads to a single
526 recruitment event in June (Colaço et al., 2006; Dixon et al., 2006). The recolonisation of *B.*
527 *azoricus* can occur through recruitment events and settlement of post-larvae and juveniles
528 or by immigration of mobile adults from nearby assemblages (Comtet and Desbruyères,
529 1998). Indeed, observations made on imagery on the Eiffel Tower edifice showed that *B.*
530 *azoricus* is able to move several centimetres a day (Matabos, Sarrazin, unpublished data).
531 Since the growth rate of *B. azoricus* juveniles has been estimated to reach ~ 2 mm per year
532 on the Eiffel Tower edifice (from imagery analysis, Sarrazin and Matabos unpublished data),
533 we can assume that the presence of mussels larger than 1 cm after 1 and 2 years of
534 recolonisation is most probably a result of adult migration. On the other hand, the mean
535 shell length of *B. azoricus* was significantly lower and a higher proportion of juveniles were
536 observed on post-disturbance assemblages compared to pre-disturbed communities. This
537 suggests that within our study, the recruitment and settlement of young mussels were the
538 main drivers of recolonisation after the disturbance, rather than migration. Moreover, the
539 results of the predator exclusion experiment suggest that the recruitment success of *B.*
540 *azoricus* might depend on predation pressure on post-larval individuals by large mobile
541 predators (e.g. shrimp, crabs, fishes). The impact of predation on the entire benthic
542 community could be even more significant when predators specifically feed on taxa that play
543 a key role in the community and interact widely with other species (Paine, 1966). We also

544 observed that the cages led to the formation of thick microbial mats on their surfaces,
545 implying that the presence of the plastic mesh and its size may have modified the input of
546 hydrothermal fluids. The deployment of additional “true” cage control quadrats would be
547 necessary to dissociate the role of predator exclusion and potentially other effects of the
548 mesh such as hydrodynamic modifications. The establishment and growth of *B. azoricus* may
549 then promote the settlement of low occurrence species and a rapid recovery of faunal
550 densities through the creation of a three dimensional habitat that contributes to reduce fluid
551 flux, making the habitat more suitable for other species (Johnson et al. 1988; Sarrazin et al.
552 1997, Shank et al. 1998). Finally, biotic interactions including predation, competition for
553 space and nutritional resources and facilitation may lead to changes in faunal relative
554 abundance and dominance before reaching an equilibrium. All these mechanisms contribute
555 to reducing the evenness among assemblages and enhance the dominance of a few taxa
556 (Fig. 9). Once this equilibrium is achieved, we can consider that these assemblages reach
557 their climax. The climax community of Montségur appears to be similar to that of the
558 neighbouring Eiffel Tower edifice (Cuvelier et al., 2011a) and some other active edifices of
559 the Lucky Strike vent field (Sarrazin et al. 2020). These communities are characterised by the
560 dominance of a few vent taxa and a high proportion of low occurrence species. Natural or
561 anthropogenic disturbance events, which can occur at each step of this successional model,
562 may lead to significant changes in faunal assemblages and even provoke community
563 collapse, depending on their spatial breadth as proposed in different vent successional
564 models (Sarrazin et al. 1997, Shank et al. 1998).

565 Several factors can come into play in recolonisation and ecological succession following a
566 disturbance, and their relative importance changes according to the scale of disturbance
567 (Zajac et al. 1998, Benedetti 2000). After a small-scale disturbance, recovery of vent
568 assemblages are strongly affected by the spatio-temporal variability of environmental
569 conditions, which may lead to local extinction or creation of new suitable habitats (Sarrazin
570 et al. 1997; Shank et al. 1998, Marcus et al. 2009; Sen et al. 2014). Feeding strategies
571 (Lelièvre et al. 2018; Van Audenhaege et al., 2019) and biotic interactions (i.e. competition
572 for space, facilitation or predation) have also been identified as important drivers of faunal
573 succession at the edifice scale (Sarrazin et al. 1997, Micheli et al. 2002; Hunt et al. 2004;
574 Govenar and Fisher 2007; Cuvelier et al. 2014a). In this study, we showed that, at this small-
575 scale, biological interactions are more likely to play a predominant role in faunal succession

576 rather than environmental conditions. The same observations have been noticed on vents at
577 back-arc basins and may be due to the high stability of environmental conditions, typical of
578 slow-spreading centers (Sen et al., 2014). Furthermore, in mosaic habitats, the diversity and
579 species composition at the boundary of disturbed patches might modulate biotic
580 interactions and migrations of individuals, influencing early stages of recovery (Bulleri et al.
581 2006). However, diversity descriptors and faunal composition were relatively homogeneous
582 between the different quadrats at each step of the recolonisation process, suggesting that
583 succession after small-scale disturbance at Lucky Strike can be described as a deterministic
584 sequence of species replacement. As observed on rocky-shore habitats, the timing of
585 disturbance might also affect recolonisation patterns (Sousa 1985, Benedetti and Cinelli
586 1996). For example, *B. azoricus* have been described to recruit seasonally around the month
587 of June (Dixon et al. 2006; Colaço et al. 2006) and the occurrence of disturbance in spring
588 might result in a faster recovery of assemblages and less importance of gastropods in the
589 first stage of recolonisation.

590

591 5. Conclusion

592 We designed a novel *in situ* experimental approach to identify biotic and abiotic factors
593 driving the recolonisation and succession of vent communities after a small-scale
594 disturbance. Recolonisation dynamics was strongly affected by species composition of the
595 neighbouring faunal assemblages. Biotic interactions were predominant and highly
596 influenced the slow recovery of vent assemblages, while environmental factors remained
597 stable. Our results, coupled with observations from literature data, lead to a first conceptual
598 model of colonisation and ecological succession for northern Mid-Atlantic communities.

599

600 At regional scales (i.e. vent field), life-history traits including reproduction (Kelly and
601 Metaxas, 2007), larval dispersal modes and recruitment abilities (Levin et al., 1996; Levin,
602 2006; Mullineaux et al., 2003, 2012) constitute additional key factors that influence faunal
603 colonisation processes and subsequent successional patterns (Zajac et al., 1998; Adams et
604 al., 2012; Nakamura et al., 2014). While the recolonisation of areas following large-scale
605 disturbance relies on dispersal across vent fields, at local scale the successful settlement of
606 post-larvae depends on habitat suitability, environmental conditions and biotic interactions.

607 Understanding the processes acting at small scales are paramount in evaluating mechanisms
608 controlling successional dynamics after recolonisation by species from afar. In addition,
609 recent workshops and working groups, emerging from the development of mining
610 regulations and the necessity to inform industries and policy makers, stressed the urgent
611 need to address knowledge gaps in vent species biology and ecology (Collins et al. 2013;
612 Levin et al. 2016; Dunn et al. 2018, ISA REMPS, SEMPIA). This study is one of the first to
613 assess natural recovery of communities on a slow-spreading ridge and provide data that are
614 essential to elaborate and develop conservation strategies and mitigate long-term harmful
615 effects of anthropogenic activities on hydrothermal vent ecosystems.

616

617 DOI of cruises involved

618 SARRADIN Pierre-Marie, CANNAT Mathilde (2017) MOMARSAT2017 cruise, RV Pourquoi pas
619 ?, <https://doi.org/10.17600/17000500>620 CANNAT Mathilde (2018) MOMARSAT2018 cruise, RV L'Atalante,
621 <https://doi.org/10.17600/18000514>622 SARRADIN Pierre-Marie, LEGRAND Julien (2019) MOMARSAT2019 cruise, RV Pourquoi pas ?,
623 <https://doi.org/10.17600/18001110>

624 Acknowledgements

625 We would like to thank the captains and crews of the oceanographic cruises Momarsat 2017,
626 2018 and 2019 aboard the vessels N/O Pourquoi pas? and L'Atalante, as well as the ROV
627 Victor6000 and Nautile team. We are particularly grateful to Pierre-Marie Sarradin and
628 Mathilde Cannat, chief scientists of the cruises who greatly supported our sampling
629 program. We are also sincerely thankful to Philippe Rodier for instrumental design of
630 pyramidal structure and cage experiment but also for the deployment of the reversing
631 thermometer and the data acquisition of bottom sea water temperature. We would like to
632 offer our special thanks to Sandra Fuchs and Fanny Girard for sample collection during the
633 cruise and Julie Tourolle for providing the map captions. We are particularly grateful for the
634 assistance given by Thomas Day, Mathilde Le Pans, Maureen Lapalme and Fanny Volage in
635 sorting and morphometrical measurements. Finally, we wish to acknowledge the help
636 provided for specimen identification by the taxonomists Dr Paulo Bonifácio and Dr Maurício
637 Shimabukuro for polychaetes, Dr Anders Warén for gastropods, Dr Inmaculada Frutos for
638 isopods, Dr Magdalena Błażewicz for tanaids, Dr Laure Corbari for amphipods and Dr Hayato
639 Tanaka for ostracods. This research was supported by the European H2020 MERCES (Project
640 ID 689518) and the eCOREF project funded by Equinor (Norway). Julien Marticorena PhD
641 project was funded by Ifremer and Equinor. This project is part of the EMSO-Azores
642 (<https://www.emso-fr.org>) regional node and EMSO ERIC Research Infrastructure
643 (<https://emso.eu/>). ERLI was supported by the European H2020 MERCES (Project ID
644 689518).

645 References

- 646 Adams, D.K., Arellano, S.M., Govenar, B., 2012. Larval dispersal : vent life in the water column.
647 <https://doi.org/10.5670/oceanog.2012.24>
- 648 Anderson, M.J., 2001. A new method for non-parametric multivariate analysis of variance. *Austral*
649 *Ecol.* 26, 32–46. <https://doi.org/10.1111/j.1442-9993.2001.01070.pp.x>
- 650 Baco, A.R., Etter, R.J., Ribeiro, P.A., Heyden, S. von der, Beerli, P., Kinlan, B.P., 2016. A synthesis of
651 genetic connectivity in deep-sea fauna and implications for marine reserve design. *Mol. Ecol.* 25,
652 3276–3298. <https://doi.org/10.1111/mec.13689>
- 653 Barreyre, T., Escartín, J., Sohn, R.A., Cannat, M., Ballu, V., Crawford, W.C., 2014. Temporal variability
654 and tidal modulation of hydrothermal exit-fluid temperatures at the Lucky Strike deep-sea vent field,
655 Mid-Atlantic Ridge. *J. Geophys. Res. Solid Earth* 119, 2543–2566.
656 <https://doi.org/10.1002/2013JB010478>
- 657 Beaulieu, S.E., Baker, E.T., German, C.R., 2015. Where are the undiscovered hydrothermal vents on
658 oceanic spreading ridges? *Deep Sea Res. Part II Top. Stud. Oceanogr., Exploring New Frontiers in*
659 *Deep-Sea Research: In Honor and Memory of Peter A. Rona* 121, 202–212.
660 <https://doi.org/10.1016/j.dsr2.2015.05.001>
- 661 Benedetti-Cecchi, L., Cinelli, F., 1996. Patterns of disturbance and recovery in littoral rock pools:
662 nonhierarchical competition and spatial variability in secondary succession. *Marine Ecology Progress*
663 *Series* 135, 145–161. <https://doi.org/10.3354/meps135145>
- 664 Benedetti-Cecchi, L., 2000. Predicting Direct and Indirect Interactions During Succession in a Mid-
665 Littoral Rocky Shore Assemblage. *Ecological Monographs* 70, 45–72. [https://doi.org/10.1890/0012-9615\(2000\)070\[0045:PDAIID\]2.0.CO;2](https://doi.org/10.1890/0012-9615(2000)070[0045:PDAIID]2.0.CO;2)
- 667 Boschen, R.E., Rowden, A.A., Clark, M.R., Gardner, J.P.A., 2013. Mining of deep-sea seafloor massive
668 sulfides: A review of the deposits, their benthic communities, impacts from mining, regulatory
669 frameworks and management strategies. *Ocean Coast. Manag.* 84, 54–67.
670 <https://doi.org/10.1016/j.ocecoaman.2013.07.005>
- 671 Breusing, C., Biastoch, A., Drews, A., Metaxas, A., Jollivet, D., Vrijenhoek, R.C., Bayer, T., Melzner, F.,
672 Sayavedra, L., Petersen, J.M., Dubilier, N., Schilabel, M.B., Rosenstiel, P., Reusch, T.B.H., 2016.
673 Biophysical and Population Genetic Models Predict the Presence of “Phantom” Stepping Stones
674 Connecting Mid-Atlantic Ridge Vent Ecosystems. *Curr. Biol. CB* 26, 2257–2267.
675 <https://doi.org/10.1016/j.cub.2016.06.062>
- 676 Bulleri, F., Benedetti-Cecchi, L., 2006. Mechanisms of recovery and resilience of different
677 components of mosaics of habitats on shallow rocky reefs. *Oecologia* 149.
678 <https://doi.org/10.1007/s00442-006-0459-3>
- 679 Butterfield, D.A., Jonasson, I.R., Massoth, G.J., Feely, R.A., Roe, K.K., Embley, R.E., Holden, J.F.,
680 McDuff, R.E., Lilley, M.D., Delaney, J.R., 1997. Seafloor eruptions and evolution of hydrothermal fluid
681 chemistry. *Philos. Trans. R. Soc. Lond. Ser. Math. Phys. Eng. Sci.* 355, 369–386.
682 <https://doi.org/10.1098/rsta.1997.0013>
- 683 Butterfield, D.A., Massoth, G.J., McDuff, R.E., Lupton, J.E., Lilley, M.D., 1990. Geochemistry of
684 hydrothermal fluids from Axial Seamount hydrothermal emissions study vent field, Juan de Fuca

- 685 Ridge: Subseafloor boiling and subsequent fluid-rock interaction. *J. Geophys. Res. Solid Earth* 95,
686 12895–12921. <https://doi.org/10.1029/JB095iB08p12895>
- 687 Chavagnac, V., Leleu, T., Fontaine, F., Cannat, M., Ceuleneer, G., Castillo, A., 2018. Spatial Variations
688 in Vent Chemistry at the Lucky Strike Hydrothermal Field, Mid-Atlantic Ridge (37°N): Updates for
689 Subseafloor Flow Geometry From the Newly Discovered Capelinhos Vent. *Geochemistry, Geophysics,*
690 *Geosystems* 19, 4444–4458. <https://doi.org/10.1029/2018GC007765>
- 691 Childress, J.J., Fisher, C.R., 1992. The biology of hydrothermal vent animals: physiology, biochemistry,
692 and autotrophic symbioses. *Unkn. J.* 337–441.
- 693 Colaço, A., Martins, I., Laranjo, M., Pires, L., Leal, C., Prieto, C., Costa, V., Lopes, H., Rosa, D., Dando,
694 P.R., Serrão-Santos, R., 2006. Annual spawning of the hydrothermal vent mussel, *Bathymodiolus*
695 *azoricus*, under controlled aquarium, conditions at atmospheric pressure. *J. Exp. Mar. Biol. Ecol.* 333,
696 166–171. <https://doi.org/10.1016/j.jembe.2005.12.005>
- 697 Collins, P.C., Kennedy, R., Van Dover, C.L., 2012. A biological survey method applied to seafloor
698 massive sulphides (sms) with contagiously distributed hydrothermal-vent fauna.
699 <https://doi.org/10.3354/meps09646>
- 700 Comtet, T., Desbruyères, D., 1998. Population structure and recruitment in mytilid bivalves from the
701 Lucky Strike and Menez Gwen hydrothermal vent fields (37°17'N and 37°50'N on the Mid-Atlantic
702 Ridge). *Mar. Ecol. Prog. Ser.* 163, 165–177. <https://doi.org/10.3354/meps163165>
- 703 Connell, J.H., Keough, M.J., 1985. Disturbance and patch dynamics of subtidal marine animals on
704 hard substrata.
- 705 Corliss, J.B., Dymond, J., Gordon, L.I., Edmond, J.M., Herzen, R.P. von, Ballard, R.D., Green, K.,
706 Williams, D., Bainbridge, A., Crane, K., Andel, T.H. van, 1979. Submarine Thermal Springs on the
707 Galápagos Rift. *Science* 203, 1073–1083. <https://doi.org/10.1126/science.203.4385.1073>
- 708 Cuvelier, D., Beesau, J., Ivanenko, V.N., Zeppilli, D., Sarradin, P.-M., Sarrazin, J., 2014a. First insights
709 into macro- and meiofaunal colonisation patterns on paired wood/slate substrata at Atlantic deep-
710 sea hydrothermal vents. *Deep Sea Res. Part Oceanogr. Res. Pap.* 87, 70–81.
711 <https://doi.org/10.1016/j.dsr.2014.02.008>
- 712 Cuvelier, D., Gollner, S., Jones, D.O.B., Kaiser, S., Arbizu, P.M., Menzel, L., Mestre, N.C., Morato, T.,
713 Pham, C., Pradillon, F., Purser, A., Raschka, U., Sarrazin, J., Simon-Lledó, E., Stewart, I.M., Stuckas, H.,
714 Sweetman, A.K., Colaço, A., 2018. Potential Mitigation and Restoration Actions in Ecosystems
715 Impacted by Seabed Mining. *Front. Mar. Sci.* 5. <https://doi.org/10.3389/fmars.2018.00467>
- 716 Cuvelier, D., Legendre, P., Laes, A., Sarradin, P.-M., Sarrazin, J., 2014b. Rhythms and Community
717 Dynamics of a Hydrothermal Tubeworm Assemblage at Main Endeavour Field – A Multidisciplinary
718 Deep-Sea Observatory Approach. *PLOS ONE* 9, e96924.
719 <https://doi.org/10.1371/journal.pone.0096924>
- 720 Cuvelier, D., Sarradin, P.-M., Sarrazin, J., Colaço, A., Copley, J.T., Desbruyères, D., Glover, A.G., Santos,
721 R.S., Tyler, P.A., 2011a. Hydrothermal faunal assemblages and habitat characterisation at the Eiffel
722 Tower edifice (Lucky Strike, Mid-Atlantic Ridge). *Mar. Ecol.* 32, 243–255.
723 <https://doi.org/10.1111/j.1439-0485.2010.00431.x>
- 724 Cuvelier, D., Sarrazin, J., Colaço, A., Copley, J., Desbruyères, D., Glover, A.G., Tyler, P., Serrão Santos,
725 R., 2009. Distribution and spatial variation of hydrothermal faunal assemblages at Lucky Strike (Mid-

- 726 Atlantic Ridge) revealed by high-resolution video image analysis. *Deep Sea Res. Part Oceanogr. Res.*
727 *Pap.* 56, 2026–2040. <https://doi.org/10.1016/j.dsr.2009.06.006>
- 728 Cuvelier, D., Sarrazin, J., Colaço, A., Copley, J.T., Glover, A.G., Tyler, P.A., Santos, R.S., Desbruyères, D.,
729 2011b. Community dynamics over 14 years at the Eiffel Tower hydrothermal edifice on the Mid-
730 Atlantic Ridge. *Limnol. Oceanogr.* 56, 1624–1640. <https://doi.org/10.4319/lo.2011.56.5.1624>
- 731 Davis, E., Becker, K., 1999. Tidal pumping of fluids within and from the oceanic crust: New
732 observations and opportunities for sampling the crustal hydrosphere. *Earth Planet. Sci. Lett.* 172,
733 141–149. [https://doi.org/10.1016/S0012-821X\(99\)00197-1](https://doi.org/10.1016/S0012-821X(99)00197-1)
- 734 Denny, M.W., 1987. Lift as a mechanism of patch initiation in mussel beds. *Journal of Experimental*
735 *Marine Biology and Ecology* 113, 231–245. [https://doi.org/10.1016/0022-0981\(87\)90103-1](https://doi.org/10.1016/0022-0981(87)90103-1)
- 736 Dixon, D.R., Lowe, D.M., Miller, P.I., Villemin, G.R., Colaço, A., Serrão-Santos, R., Dixon, L.R.J., 2006.
737 Evidence of seasonal reproduction in the Atlantic vent mussel *Bathymodiolus azoricus*, and an
738 apparent link with the timing of photosynthetic primary production. *J. Mar. Biol. Assoc. U. K.* 86,
739 1363–1371. <https://doi.org/10.1017/S0025315406014391>
- 740 Donval, J.-P., Charlou, J.-L., Lucas, L., 2008. Analysis of light hydrocarbons in marine sediments by
741 headspace technique: Optimization using design of experiments. *Chemometrics and Intelligent*
742 *Laboratory Systems* 94, 89–94. <https://doi.org/10.1016/j.chemolab.2008.06.010>
- 743 Dray, S., Bauman, D., Blanchet, G., Borcard, D., Clappe, S., Guenard, G., Jombart, T., Larocque, G.,
744 Legendre, P., Madi, N., Wagner, H.H., 2020. *adespatial: Multivariate Multiscale Spatial Analysis*.
- 745 Dreyer, J.C., Knick, K.E., Flickinger, W.B., Dover, C.L.V., 2005. Development of macrofaunal
746 community structure in mussel beds on the northern East Pacific Rise. *Mar. Ecol. Prog. Ser.* 302, 121–
747 134. <https://doi.org/10.3354/meps302121>
- 748 Dunn, D.C., Dover, C.L.V., Etter, R.J., Smith, C.R., Levin, L.A., Morato, T., Colaço, A., Dale, A.C., Gebruk,
749 A.V., Gjerde, K.M., Halpin, P.N., Howell, K.L., Johnson, D., Perez, J.A.A., Ribeiro, M.C., Stuckas, H.,
750 Weaver, P., Participants, S.W., 2018. A strategy for the conservation of biodiversity on mid-ocean
751 ridges from deep-sea mining. *Science Advances* 4, eaar4313. <https://doi.org/10.1126/sciadv.aar4313>
- 752 Kassambara and Mundt, 2009. *Factoextra: Extract and Visualize the Results of Multivariate Data*
753 *Analyses*, 2019. , R package.
- 754 Gollner, S., Govenar, B., Arbizu, P.M., Mills, S., Le Bris, N., Weinbauer, M., Shank, T.M., Bright, M.,
755 2015a. Differences in recovery between deep-sea hydrothermal vent and vent-proximate
756 communities after a volcanic eruption. *Deep Sea Res. Part Oceanogr. Res. Pap.* 106, 167–182.
757 <https://doi.org/10.1016/j.dsr.2015.10.008>
- 758 Gollner, S., Riemer, B., Arbizu, P.M., Bris, N.L., Bright, M., 2010. Diversity of Meiofauna from the
759 9°50'N East Pacific Rise across a Gradient of Hydrothermal Fluid Emissions. *PLOS ONE* 5, e12321.
760 <https://doi.org/10.1371/journal.pone.0012321>
- 761 Gollner, S., Govenar, B., Fisher, C.R., Bright, M., 2015b. Size matters at deep-sea hydrothermal vents:
762 different diversity and habitat fidelity patterns of meio- and macrofauna. *Mar. Ecol. Prog. Ser.* 520,
763 57–66. <https://doi.org/10.3354/meps11078>
- 764 Gollner, S., Kaiser, S., Menzel, L., Jones, D.O.B., Brown, A., Mestre, N.C., van Oevelen, D., Menot, L.,
765 Colaço, A., Canals, M., Cuvelier, D., Durden, J.M., Gebruk, A., Egho, G.A., Haeckel, M., Marcon, Y.,
766 Mevenkamp, L., Morato, T., Pham, C.K., Purser, A., Sanchez-Vidal, A., Vanreusel, A., Vink, A., Martinez

- 767 Arbizu, P., 2017. Resilience of benthic deep-sea fauna to mining activities. *Mar. Environ. Res.* 129,
768 76–101. <https://doi.org/10.1016/j.marenvres.2017.04.010>
- 769 Gollner, S., Govenar, B., Martinez Arbizu, P., Mullineaux, L.S., Mills, S., Le Bris, N., Weinbauer, M.,
770 Shank, T.M., Bright, M., 2020. Animal Community Dynamics at Senescent and Active Vents at the 9°N
771 East Pacific Rise After a Volcanic Eruption. *Front. Mar. Sci.* 6.
772 <https://doi.org/10.3389/fmars.2019.00832>
- 773 Govenar, B., Fisher, C.R., 2007. Experimental evidence of habitat provision by aggregations of *Riftia*
774 *pachytila* at hydrothermal vents on the East Pacific Rise. *Mar. Ecol.* 28, 3–14.
775 <https://doi.org/10.1111/j.1439-0485.2007.00148.x>
- 776 Hunt, H.L., Metaxas, A., Jennings, R.M., Halanych, K.M., Mullineaux, L.S., 2004. Testing biological
777 control of colonization by vestimentiferan tubeworms at deep-sea hydrothermal vents (East Pacific
778 Rise, 9°50'N). *Deep Sea Res. Part Oceanogr. Res. Pap.* 51, 225–234.
779 <https://doi.org/10.1016/j.dsr.2003.10.008>
- 780 Husson, B., Sarradin, P.-M., Zeppilli, D., Sarrazin, J., 2017. Picturing thermal niches and biomass of
781 hydrothermal vent species. *Deep Sea Res. Part II Top. Stud. Oceanogr., Advances in deep-sea biology:*
782 *biodiversity, ecosystem functioning and conservation* 137, 6–25.
783 <https://doi.org/10.1016/j.dsr2.2016.05.028>
- 784 Johnson, K.S., Childress, J.J., Beehler, C.L., 1988. Short-term temperature variability in the Rose
785 Garden hydrothermal vent field: an unstable deep-sea environment. *Deep Sea Res. Part Oceanogr.*
786 *Res. Pap.* 35, 1711–1721. [https://doi.org/10.1016/0198-0149\(88\)90045-3](https://doi.org/10.1016/0198-0149(88)90045-3)
- 787 Jollivet, D., Empis, A., Baker, M.C., Hourdez, S., Comtet, T., Jouin-Toulmond, C., Desbruyères, D.,
788 Tyler, P.A., 2000. Reproductive biology, sexual dimorphism, and population structure of the deep sea
789 hydrothermal vent scale-worm, *Branchipolynoe seepensis* (Polychaeta: Polynoidae). *Journal of the*
790 *Marine Biological Association of the United Kingdom* 80, 55–68.
791 <https://doi.org/10.1017/S0025315499001563>
- 792 Kelly, N.E., Metaxas, A., 2007. Influence of habitat on the reproductive biology of the deep-sea
793 hydrothermal vent limpet *Lepetodrilus fucensis* (Vetigastropoda: Mollusca) from the Northeast
794 Pacific. *Mar. Biol.* 151, 649–662. <https://doi.org/10.1007/s00227-006-0505-z>
- 795 Khripounoff, A., Vangriesheim, A., Crassous, P., Segonzac, M., Lafon, V., Warén, A., 2008. Temporal
796 variation of currents, particulate flux and organism supply at two deep-sea hydrothermal fields of the
797 Azores Triple Junction. *Deep Sea Res. Part Oceanogr. Res. Pap.* 55, 532–551.
798 <https://doi.org/10.1016/j.dsr.2008.01.001>
- 799 Langmuir, C., Humphris, S., Fornari, D., Van Dover, C., Von Damm, K., Tivey, M.K., Colodner, D.,
800 Charlou, J.-L., Desonie, D., Wilson, C., Fouquet, Y., Klinkhammer, G., Bougault, H., 1997.
801 Hydrothermal vents near a mantle hot spot: the Lucky Strike vent field at 37°N on the Mid-Atlantic
802 Ridge. *Earth Planet. Sci. Lett.* 148, 69–91. [https://doi.org/10.1016/S0012-821X\(97\)00027-7](https://doi.org/10.1016/S0012-821X(97)00027-7)
- 803 Le Bris, N., Govenar, B., Le Gall, C., Fisher, C.R., 2006. Variability of physico-chemical conditions in
804 9°50'N EPR diffuse flow vent habitats. *Mar. Chem.* 98, 167–182.
805 <https://doi.org/10.1016/j.marchem.2005.08.008>
- 806 Leibold, M.A., Holyoak, M., Mouquet, N., Amarasekare, P., Chase, J.M., Hoopes, M.F., Holt, R.D.,
807 Shurin, J.B., Law, R., Tilman, D., Loreau, M., Gonzalez, A., 2004. The metacommunity concept: a

- 808 framework for multi-scale community ecology. *Ecology Letters* 7, 601–613.
809 <https://doi.org/10.1111/j.1461-0248.2004.00608.x>
- 810 Lelièvre, Y., Legendre, P., Matabos, M., Mihály, S., Lee, R.W., Sarradin, P.-M., Arango, C.P., Sarrazin,
811 J., 2017. Astronomical and atmospheric impacts on deep-sea hydrothermal vent invertebrates. *Proc.*
812 *R. Soc. B Biol. Sci.* 284, 319–407. <https://doi.org/10.1098/rspb.2016.2123>
- 813 Lenihan, H.S., Mills, S.W., Mullineaux, L.S., Peterson, C.H., Fisher, C.R., Micheli, F., 2008. Biotic
814 interactions at hydrothermal vents: Recruitment inhibition by the mussel *Bathymodiolus*
815 *thermophilus*. *Deep Sea Res. Part Oceanogr. Res. Pap.* 55, 1707–1717.
816 <https://doi.org/10.1016/j.dsr.2008.07.007>
- 817 Levin, L.A., 2006. Recent progress in understanding larval dispersal: new directions and digressions.
818 *Integr. Comp. Biol.* 46, 282–297. <https://doi.org/10.1093/icb/icj024>
- 819 Levin, L.A., Baco, A.R., Bowden, D.A., Colaco, A., Cordes, E.E., Cunha, M.R., Demopoulos, A.W.J.,
820 Gobin, J., Grupe, B.M., Le, J., Metaxas, A., Netburn, A.N., Rouse, G.W., Thurber, A.R., Tunnicliffe, V.,
821 Van Dover, C.L., Vanreusel, A., Watling, L., 2016a. Hydrothermal Vents and Methane Seeps:
822 Rethinking the Sphere of Influence. *Front. Mar. Sci.* 3. <https://doi.org/10.3389/fmars.2016.00072>
- 823 Levin, L.A., D, T., G, T., 1996. Succession of macrobenthos in a created salt marsh. *Mar. Ecol. Prog.*
824 *Ser.* 141, 67–82. <https://doi.org/10.3354/meps141067>
- 825 Levin, L.A., Mengerink, K., Gjerde, K.M., Rowden, A.A., Van Dover, C.L., Clark, M.R., Ramirez-Llodra,
826 E., Currie, B., Smith, C.R., Sato, K.N., Gallo, N., Sweetman, A.K., Lily, H., Armstrong, C.W., Brier, J.,
827 2016b. Defining “serious harm” to the marine environment in the context of deep-seabed mining.
828 *Mar. Policy* 74, 245–259. <https://doi.org/10.1016/j.marpol.2016.09.032>
- 829 Luther, G.W., Rozan, T.F., Taillefert, M., Nuzzio, D.B., Di Meo, C., Shank, T.M., Lutz, R.A., Cary, S.C.,
830 2001. Chemical speciation drives hydrothermal vent ecology. *Nature* 410, 813–816.
831 <https://doi.org/10.1038/35071069>
- 832 Marcus, J., Tunnicliffe, V., Butterfield, D.A., 2009. Post-eruption succession of macrofaunal
833 communities at diffuse flow hydrothermal vents on Axial Volcano, Juan de Fuca Ridge, Northeast
834 Pacific. *Deep Sea Res. Part II Top. Stud. Oceanogr., Marine Benthic Ecology and Biodiversity: A*
835 *Compilation of Recent Advances in Honor of J. Frederick Grassle* 56, 1586–1598.
836 <https://doi.org/10.1016/j.dsr2.2009.05.004>
- 837 Marsh, L., Copley, J.T., Huvenne, V.A.I., Linse, K., Reid, W.D.K., Rogers, A.D., Sweeting, C.J., Tyler, P.A.,
838 2012. Microdistribution of Faunal Assemblages at Deep-Sea Hydrothermal Vents in the Southern
839 Ocean. *PLoS One* 7. <https://doi.org/10.1371/journal.pone.0048348>
- 840 Marticorena, J., Matabos, M., Sarrazin, J., Ramirez-Llodra, E., 2020. Contrasting reproductive biology
841 of two hydrothermal gastropods from the Mid-Atlantic Ridge: implications for resilience of vent
842 communities. *Mar. Biol.* 167, 109. <https://doi.org/10.1007/s00227-020-03721-x>
- 843 Mat, A.M., Sarrazin, J., Markov, G.V., Apremont, V., Dubreuil, C., Eché, C., Fabioux, C., Klopp, C.,
844 Sarradin, P.-M., Tanguy, A., Huvet, A., Matabos, M., 2020. Biological rhythms in the deep-sea
845 hydrothermal mussel *Bathymodiolus azoricus*. *Nature Communications* 11, 3454.
846 <https://doi.org/10.1038/s41467-020-17284-4>

- 847 Micheli, F., Peterson, C.H., Mullineaux, L.S., Fisher, C.R., Mills, S.W., Sancho, G., Johnson, G.A.,
848 Lenihan, H.S., 2002. Predation Structures Communities at Deep-Sea Hydrothermal Vents. *Ecol.*
849 *Monogr.* 72, 365–382. [https://doi.org/10.1890/0012-9615\(2002\)072\[0365:PSCADS\]2.0.CO;2](https://doi.org/10.1890/0012-9615(2002)072[0365:PSCADS]2.0.CO;2)
- 850 Mullineaux, L.S., Adams, D.K., Mills, S.W., Beaulieu, S.E., 2010. Larvae from afar colonize deep-sea
851 hydrothermal vents after a catastrophic eruption. *Proc. Natl. Acad. Sci.* 107, 7829–7834.
852 <https://doi.org/10.1073/pnas.0913187107>
- 853 Mullineaux, L.S., Metaxas, A., Beaulieu, S.E., Bright, M., Gollner, S., Grupe, B.M., Herrera, S., Kellner,
854 J.B., Levin, L.A., Mitarai, S., Neubert, M.G., Thurnherr, A.M., Tunnicliffe, V., Watanabe, H.K., Won, Y.-
855 J., 2018. Exploring the Ecology of Deep-Sea Hydrothermal Vents in a Metacommunity Framework.
856 *Front. Mar. Sci.* 5. <https://doi.org/10.3389/fmars.2018.00049>
- 857 Mullineaux, L.S., Bris, N.L., Mills, S.W., Henri, P., Bayer, S.R., Secrist, R.G., Siu, N., 2012. Detecting the
858 Influence of Initial Pioneers on Succession at Deep-Sea Vents. *PLOS ONE* 7, e50015.
859 <https://doi.org/10.1371/journal.pone.0050015>
- 860 Mullineaux, L.S., Peterson, C.H., Micheli, F., Mills, S.W., 2003. Successional Mechanism Varies Along a
861 Gradient in Hydrothermal Fluid Flux at Deep-Sea Vents. *Ecol. Monogr.* 73, 523–542.
862 <https://doi.org/10.1890/02-0674>
- 863 Nakamura, M., Watanabe, H., Sasaki, T., Ishibashi, J., Fujikura, K., Mitarai, S., 2014. Life history traits
864 of *Lepetodrilus nux* in the Okinawa Trough, based upon gametogenesis, shell size, and genetic
865 variability. *Mar. Ecol. Prog. Ser.* 505, 119–130. <https://doi.org/10.3354/meps10779>
- 866 Oksanen, J., Blanchet, F.G., Friendly, M., Kindt, R., Legendre, P., McGlenn, D., Minchin, P.R., O'Hara,
867 R.B., Simpson, G.L., Solymos, P., Stevens, M.H.H., Szoecs, E., Wagner, H., 2019. *vegan: Community*
868 *Ecology Package.*
- 869 Ondreas, H., Cannat, M., Fouquet, Y., Normand, A., Sarradin, P., Sarrazin, J., 2009. Recent volcanic
870 events and the distribution of hydrothermal venting at the Lucky Strike hydrothermal field, Mid-
871 Atlantic Ridge. *Geochem. Geophys. Geosystems* 10. <https://doi.org/10.1029/2008gc002171>
- 872 Orcutt, B.N., Bradley, J.A., Brazelton, W.J., Estes, E.R., Goordial, J.M., Huber, J.A., Jones, R.M.,
873 Mahmoudi, N., Marlow, J.J., Murdock, S., Pachiadaki, M., 2020. Impacts of deep-sea mining on
874 microbial ecosystem services. *Limnol. Oceanogr.* n/a. <https://doi.org/10.1002/lno.11403>
- 875 Paine, R.T., 1966. Food Web Complexity and Species Diversity. *Am. Nat.* 100, 65–75.
- 876 Sancho, G., Fisher, C.R., Mills, S., Micheli, F., Johnson, G.A., Lenihan, H.S., Peterson, C.H., Mullineaux,
877 L.S., 2005. Selective predation by the zoarcid fish *Thermarces cerberus* at hydrothermal vents. *Deep*
878 *Sea Res. Part Oceanogr. Res. Pap.* 52, 837–844. <https://doi.org/10.1016/j.dsr.2004.12.002>
- 879 Sarradin, P.-M., Waeles, M., Bernagout, S., Le Gall, C., Sarrazin, J., Riso, R., 2009. Speciation of
880 dissolved copper within an active hydrothermal edifice on the Lucky Strike vent field (MAR, 37°N).
881 *Sci. Total Environ.* 407, 869–878. <https://doi.org/10.1016/j.scitotenv.2008.09.056>
- 882 Sarrazin, J., Cuvelier, D., Peton, L., Legendre, P., Sarradin, P.M., 2014. High-resolution dynamics of a
883 deep-sea hydrothermal mussel assemblage monitored by the EMSO-Açores MoMAR observatory.
884 *Deep Sea Res. Part Oceanogr. Res. Pap.* 90, 62–75. <https://doi.org/10.1016/j.dsr.2014.04.004>
- 885 Sarrazin, J., Levesque, C., Juniper, S., Tivey, M., 2002. Mosaic community dynamics on Juan de Fuca
886 Ridge sulphide edifices: substratum, temperature and implications for trophic structure. *CBM -*
887 *Cahiers de Biologie Marine* 43, 275–279.

- 888 Sarrazin, J., Juniper, S.K., Massoth, G., Legendre, P., 1999. Physical and chemical factors influencing
889 species distributions on hydrothermal sulfide edifices of the Juan de Fuca Ridge, northeast Pacific.
890 *Mar. Ecol. Prog. Ser.* 190, 89–112. <https://doi.org/10.3354/meps190089>
- 891 Sarrazin, J., Legendre, P., de Busserolles, F., Fabri, M.-C., Guilini, K., Ivanenko, V.N., Morineaux, M.,
892 Vanreusel, A., Sarradin, P.-M., 2015a. Biodiversity patterns, environmental drivers and indicator
893 species on a high-temperature hydrothermal edifice, Mid-Atlantic Ridge. *Deep Sea Res. Part II Top.*
894 *Stud. Oceanogr.*, Exploring New Frontiers in Deep-Sea Research: In Honor and Memory of Peter A.
895 Rona 121, 177–192. <https://doi.org/10.1016/j.dsr2.2015.04.013>
- 896 Sarrazin, J., Portail, M., Legrand, E., Cathalot, C., Laes, A., Lahaye, N., Sarradin, P.M., Husson, B., 2020.
897 Endogenous versus exogenous factors: What matters for vent mussel communities? *Deep Sea Res.*
898 *Part Oceanogr. Res. Pap.* 103260. <https://doi.org/10.1016/j.dsr.2020.103260>
- 899 Sarrazin, J., V, R., Sk, J., Jr, D., 1997. Biological and geological dynamics over four years on a high-
900 temperature sulfide structure at the Juan de Fuca Ridge hydrothermal observatory. *Mar. Ecol. Prog.*
901 *Ser.* 153, 5–24. <https://doi.org/10.3354/meps153005>
- 902 Scheirer, D.S., Shank, T.M., Fornari, D.J., 2006. Temperature variations at diffuse and focused flow
903 hydrothermal vent sites along the northern East Pacific Rise. *Geochem. Geophys. Geosystems* 7.
904 <https://doi.org/10.1029/2005GC001094>
- 905 Sen, A., Becker, E.L., Podowski, E.L., Wickes, L.N., Ma, S., Mullaugh, K.M., Hourdez, S., Luther, G.W.,
906 Fisher, C.R., 2013. Distribution of mega fauna on sulfide edifices on the Eastern Lau Spreading Center
907 and Valu Fa Ridge. *Deep Sea Res. Part Oceanogr. Res.* 72, 48–60.
908 <https://doi.org/10.1016/j.dsr.2012.11.003>
- 909 Sen, A., Podowski, E.L., Becker, E.L., Shearer, E.A., Gartman, A., Yücel, M., Hourdez, S., Luther, G.W.,
910 III, Fisher, C.R., 2014. Community succession in hydrothermal vent habitats of the Eastern Lau
911 Spreading Center and Valu Fa Ridge, Tonga. *Limnol. Oceanogr.* 59, 1510–1528.
912 <https://doi.org/10.4319/lo.2014.59.5.1510>
- 913 Shank, T.M., Fornari, D.J., Von Damm, K.L., Lilley, M.D., Haymon, R.M., Lutz, R.A., 1998. Temporal and
914 spatial patterns of biological community development at nascent deep-sea hydrothermal vents
915 (9°50'N, East Pacific Rise). *Deep Sea Res. Part II Top. Stud. Oceanogr.* 45, 465–515.
916 [https://doi.org/10.1016/S0967-0645\(97\)00089-1](https://doi.org/10.1016/S0967-0645(97)00089-1)
- 917 Sousa, W.P., 1985. Disturbance and patch dynamics on rocky intertidal shores. The ecology of natural
918 disturbance and patch dynamics.
- 919 Spiess, F.N., Macdonald, K.C., Atwater, T., Ballard, R., Carranza, A., Cordoba, D., Cox, C., Garcia, V.M.,
920 Francheteau, J., Guerrero, J., Hawkins, J., Haymon, R., Hessler, R., Juteau, T., Kastner, M., Larson, R.,
921 Luyendyk, B., Macdougall, J.D., Miller, S., Normark, W., Orcutt, J., Rangin, C., 1980. East pacific rise:
922 hot springs and geophysical experiments. *Science* 207, 1421–1433.
923 <https://doi.org/10.1126/science.207.4438.1421>
- 924 Suzuki, K., Yoshida, K., Watanabe, H., Yamamoto, H., 2018. Mapping the resilience of chemosynthetic
925 communities in hydrothermal vent fields. *Sci. Rep.* 8, 9364. [https://doi.org/10.1038/s41598-018-](https://doi.org/10.1038/s41598-018-27596-7)
926 [27596-7](https://doi.org/10.1038/s41598-018-27596-7)
- 927 Tengberg, A., Hovdenes, J., Andersson, H.J., Brocandel, O., Diaz, R., Hebert, D., Arnerich, T., Huber, C.,
928 Körtzinger, A., Khripounoff, A., Rey, F., Rønning, C., Schimanski, J., Sommer, S., Stangelmayer, A.,

- 929 2006. Evaluation of a lifetime-based optode to measure oxygen in aquatic systems. *Limnology and*
930 *Oceanography: Methods* 4, 7–17. <https://doi.org/10.4319/lom.2006.4.7>
- 931 Tolstoy, M., Cowen, J.P., Baker, E.T., Fornari, D.J., Rubin, K.H., Shank, T.M., Waldhauser, F.,
932 Bohnenstiehl, D.R., Forsyth, D.W., Holmes, R.C., Love, B., Perfit, M.R., Weekly, R.T., Soule, S.A.,
933 Glazer, B., 2006. A Sea-Floor Spreading Event Captured by Seismometers. *Science* 314, 1920–1922.
934 <https://doi.org/10.1126/science.1133950>
- 935 Tunnicliffe, V., 1991. The biology of hydrothermal vents : ecology and evolution. *Biol. Hydrothermal*
936 *Vents Ecol. Evol.* 29, 319–407.
- 937 Tunnicliffe, V., Embley, R.W., Holden, J.F., Butterfield, D.A., Massoth, G.J., Juniper, S.K., 1997.
938 Biological colonization of new hydrothermal vents following an eruption on Juan de Fuca Ridge. *Deep*
939 *Sea Res. Part Oceanogr. Res. Pap.* 44, 1627–1644. [https://doi.org/10.1016/S0967-0637\(97\)00041-1](https://doi.org/10.1016/S0967-0637(97)00041-1)
- 940 Van Audenhaege, L., Fariñas-Bermejo, A., Schultz, T., Lee Van Dover, C., 2019. An environmental
941 baseline for food webs at deep-sea hydrothermal vents in Manus Basin (Papua New Guinea). *Deep*
942 *Sea Res. Part Oceanogr. Res. Pap.* 148, 88–99. <https://doi.org/10.1016/j.dsr.2019.04.018>
- 943 Van Dover, C.L., 2007. The biological environment of polymetallic sulphides deposits, the potential
944 impact of exploration and mining on this environment, and data required to establish environmental
945 baselines in exploration areas. In: *Polymetallic Sulphides and Cobalt-rich Ferromanganese Crusts*
946 *Deposits: Establishment of Environmental Baselines and an Associated Monitoring Programme*
947 *during Exploration. Proceedings of the International Seabed Authority's Workshop held in Kingston,*
948 *Jamaica, 6e10 September 2004. Prepared by Offices of Resources and Environmental Monitoring*
949 *(OREM), pp. 169e190. International Seabed Authority, Kingston, Jamaica:*
950 [http://www.isa.org.jm/files/](http://www.isa.org.jm/files/documents/EN/Workshops/2004/Proceedings-ae.pdf)
951 [documents/EN/Workshops/2004/Proceedings-ae.pdf](http://www.isa.org.jm/files/documents/EN/Workshops/2004/Proceedings-ae.pdf). (accessed
13.06.13.).
- 952 Van Dover, C.L., 2011. Mining seafloor massive sulphides and biodiversity: what is at risk? *ICES J.*
953 *Mar. Sci.* 68, 341–348. <https://doi.org/10.1093/icesjms/fsq086>
- 954 Van Dover, C.L., 2010. Mining seafloor massive sulphides and biodiversity: what is at risk? *ICES J.*
955 *Mar. Sci.* 68, 341–348. <https://doi.org/10.1093/icesjms/fsq086>
- 956 Vuillemin, R., Le Roux, D., Dorval, P., Bucas, K., Sudreau, J.P., Hamon, M., Le Gall, C., Sarradin, P.M.,
957 2009. CHEMINI: A new in situ CHEmical MINIaturized analyzer. *Deep Sea Res. Part Oceanogr. Res.*
958 *Pap.* 56, 1391–1399. <https://doi.org/10.1016/j.dsr.2009.02.002>
- 959 Washburn, T.W., Turner, P.J., Durden, J.M., Jones, D.O.B., Weaver, P., Van Dover, C.L., 2019.
960 Ecological risk assessment for deep-sea mining. *Ocean Coast. Manag.* 176, 24–39.
961 <https://doi.org/10.1016/j.ocecoaman.2019.04.014>
- 962 Zajac, R.N., Whitlatch, R.B., Thrush, S.F., 1998. Recolonization and succession in soft-sediment
963 infaunal communities: the spatial scale of controlling factors. *Hydrobiologia* 375, 227–240.
964 <https://doi.org/10.1023/A:1017032200173>

Table 1. Environmental conditions on the baseline communities of the different quadrats deployed on the Montségur edifice (Lucky Strike vent field, Mid-Atlantic Ridge). Temperature: average: T.avg., standard deviation: T.std. maximum: T.max and minimum: T.min. from iButtonsTM. Oxygen (O₂). Total dissolved sulphide (TdS) and Total dissolved iron (TdFe) measured with the in situ analysers CHEMINI. Methane (CH₄) and pH were measured through quantitative analyses from samples collected with the PEPITO water sampler (Sarradin et al. 2009). Highest values are highlighted in bold and lowest values in grey.

Quadrat

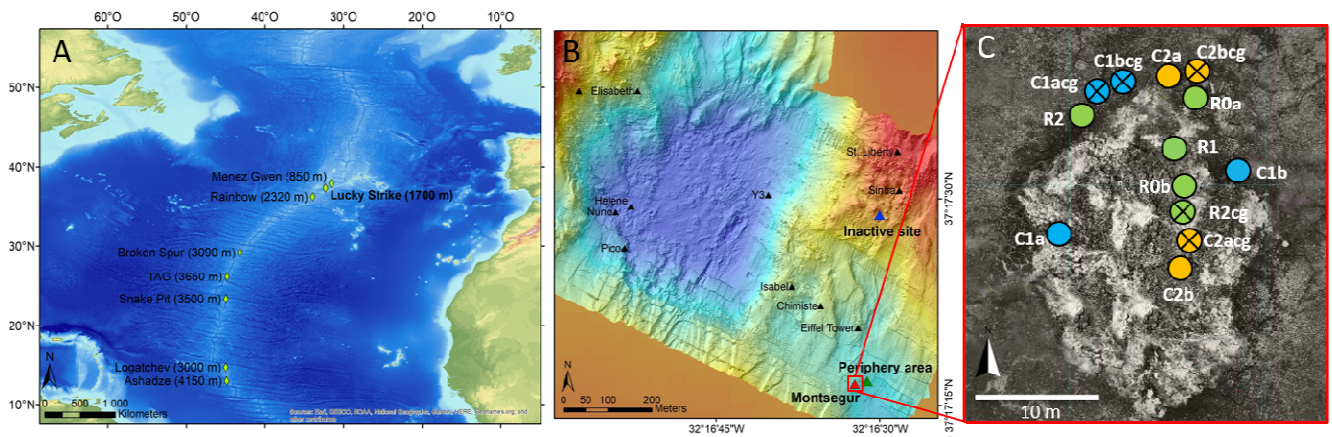


Figure 1. **A.** Location of the Lucky Strike (LS) vent field along the Mid-Atlantic Ridge. **B.** Bathymetric chart of LS and location of the Montségur edifice **C.** Position of the experimental and reference quadrats on and around the Montségur edifice. Green circles represent the reference quadrats, blue circles represent the experimental quadrats used to study the recolonisation 1 year after the disturbance, and orange circles represent the experimental quadrats used to study the recolonisation 2 years after the disturbance. Crossed off circles represent “caged” quadrats while empty circles represent quadrats without a cage.

Figure 2. The C1a-cg experimental quadrat in 2017, (A) before faunal clearance (baseline community) and ; (B) after the induced disturbance. Red arrow highlights the check-board used to calibrate imagery analysis and estimate the sampling surface area (red dotted line). (C) The C1bcg “caged” experimental quadrat used to exclude large mobile predators. A 1 cm mesh grid was adjusted on the pyramidal structure on top of the quadrat (in black on the picture) and a grey fabric sleeve was attached to the edge of the caged quadrat to avoid colonisation of crawlers. A camera was deployed at the top of the pyramidal structure and connected to a battery on the side (yellow cables).

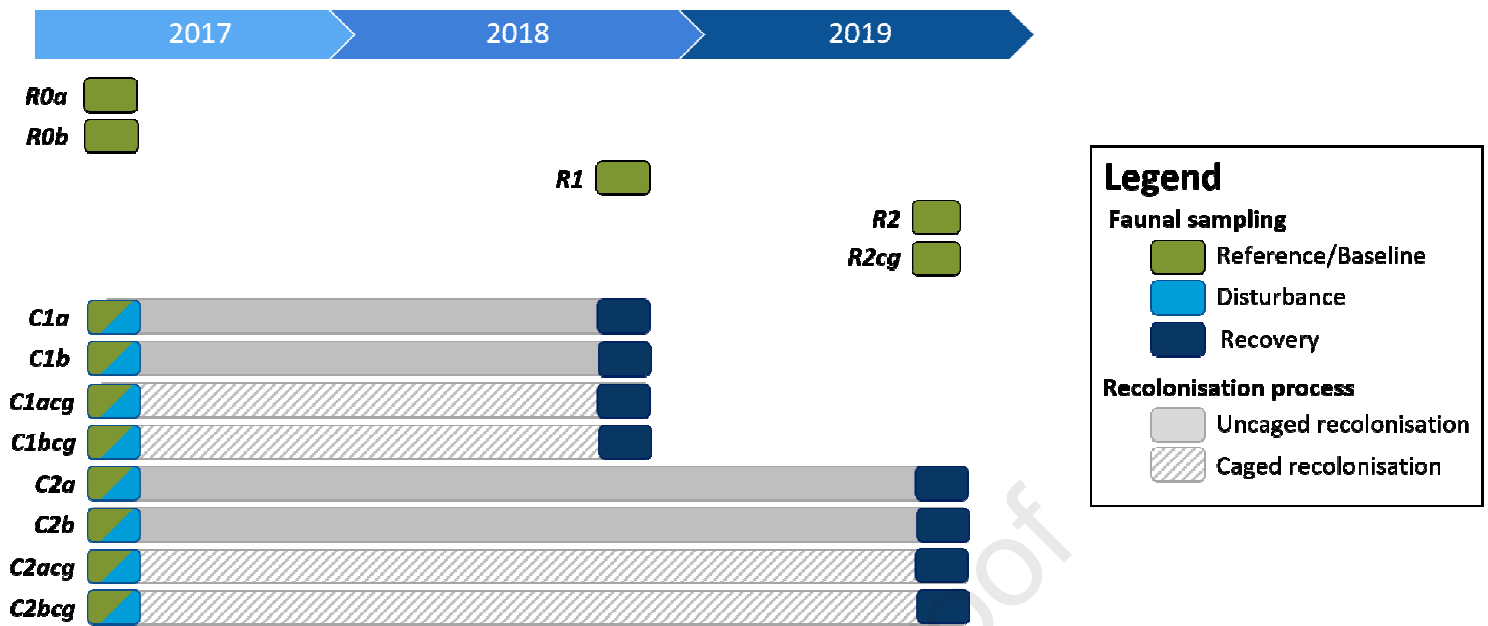


Figure 3. Experimental design of the disturbance experiment deployed between 2017 and 2019 on the Montségur edifice, Lucky Strike vent field (Mid-Atlantic Ridge). Small rectangles represent faunal sampling and their color indicates the nature of the operation: green, sampling of baseline communities; light blue, induction of disturbance by clearing faunal assemblages; dark blue, sampling after recolonisation to evaluate the recovery. Grey segments represent the recolonisation period studied for each quadrat. Hatched segments indicate the presence of cages during the recolonisation period.

Figure 4. Species richness (a), total density (b), Shannon index (c) and Pielou's evenness index (d) of macrofaunal communities on the baseline communities and during the recolonisation process on the active Montségur edifice. Pre: assemblages sampled before the disturbance; Post1: assemblages sampled 1 year after the disturbance; Post2: assemblages sampled 2 years after the disturbance. Significance of Kruskal-Wallis multisample tests and post-hoc Dunn's tests are represented on the top of the boxplots.

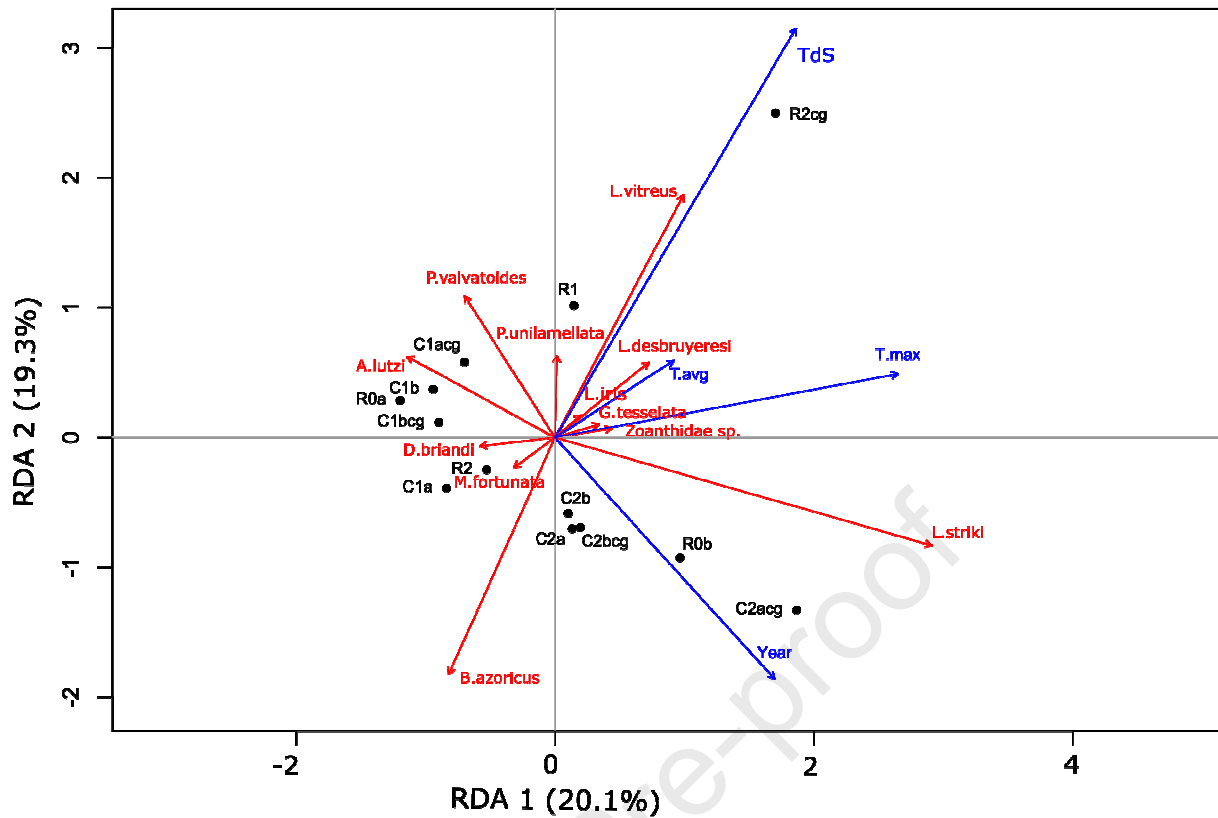


Figure 5. Canonical redundancy analysis (RDA, scaling 2) of Hellinger-transformed macrofaunal densities observed in the baseline community of the Montségur active edifice at the Lucky Strike vent field (Mid-Atlantic Ridge). The first canonical axis represents 20.1 % of the total variance in macrofaunal densities while the second axis represents 19.3% (adj $R^2 = 25.1\%$, $p = 0.004$). The first axis is significant ($p = 0.05$). Only species that accounted for more than 50% of cumulative inertia on the two first axes are represented.

Figure 6. Histograms and boxplots of size frequency distribution of *Bathymodiolus azoricus* for each quadrat sampled at the Montségur edifice at the Lucky Strike vent field (Mid-Atlantic Ridge) including the pre-disturbed community (blue) and the communities one (red) and 2 (green) years after disturbance. Wilcoxon-Mann-Whitney tests were performed to identify differences in mean individual size between the baseline and post-disturbance communities. Asterisks indicate significant differences in mean shell length (*p-value<0.05; ** p-value <0.01; *** p-value <0.001). The interval between dotted lines represents the range of size at recruitment. The percentages represent the proportion of *B. azoricus* density which recovered in comparison of the pre-disturbed value in each quadrat.

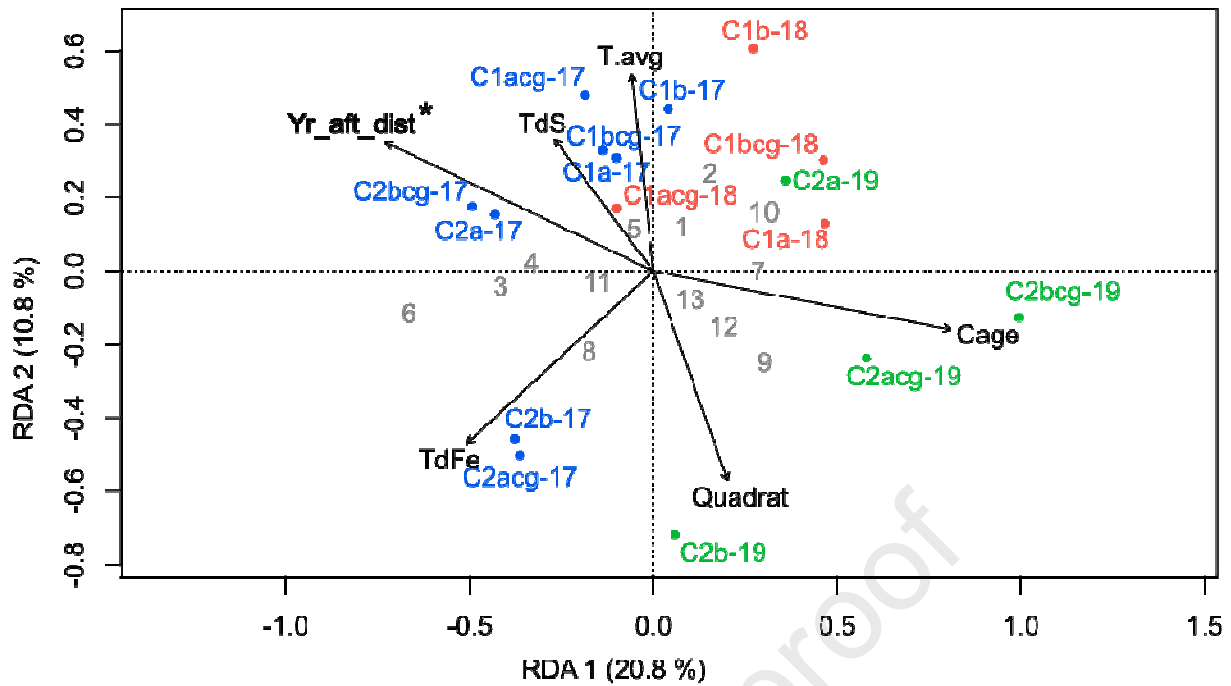


Figure 7. Canonical redundancy analysis (RDA, scaling 2) of Hellinger-transformed macrofaunal densities observed in the different assemblages during the recolonization process at the Montségur active edifice (Lucky Strike vent field, Mid-Atlantic Ridge). The first canonical axis represents 20.8% of the total variance in macrofaunal densities while the second axis represents 10.8% (with an adjusted R^2 of 20.5%). The RDA and the first axis are significant (p -values = 0.006 and 0.023, respectively). Only species showing good fit with the first two canonical axes are represented. Colors refer to the time after disturbance: baseline communities (blue); 1 year after disturbance (red); two years after disturbance (green). Explanatory variables: Years after disturbance (Yr_aft_dist), average temperature measured before sampling (T.avg), mean concentration of total dissolved sulphides (TdS), mean concentration of total dissolved iron (TdFe), if quadrats are caged or uncaged (Cage), identification of quadrats to test the dependence of the same location over the time of the experiment (Quadrat). Response variables, each species is designated by a number: 1 – *Amphisamytha lutzi*; 2 – *Aphotopontius* sp.; 3 – *Bathymodiolus azoricus*; 4 – *Branchipolynoe seepensis*; 5 – *Lepetodrilus atlanticus*; 6 – *Lirapex costellata*; 7 – *Laeviphitus desbruyeresi*; 8 – *Luckia striki*; 9 – *Lurifax vitreus*; 10 – *Oncholaimus dyvae*; 11 – *Paralepetopsis ferrugivora*; 12 – *Protolira valvatoides*; 13 – *Xylodiscula analoga*.

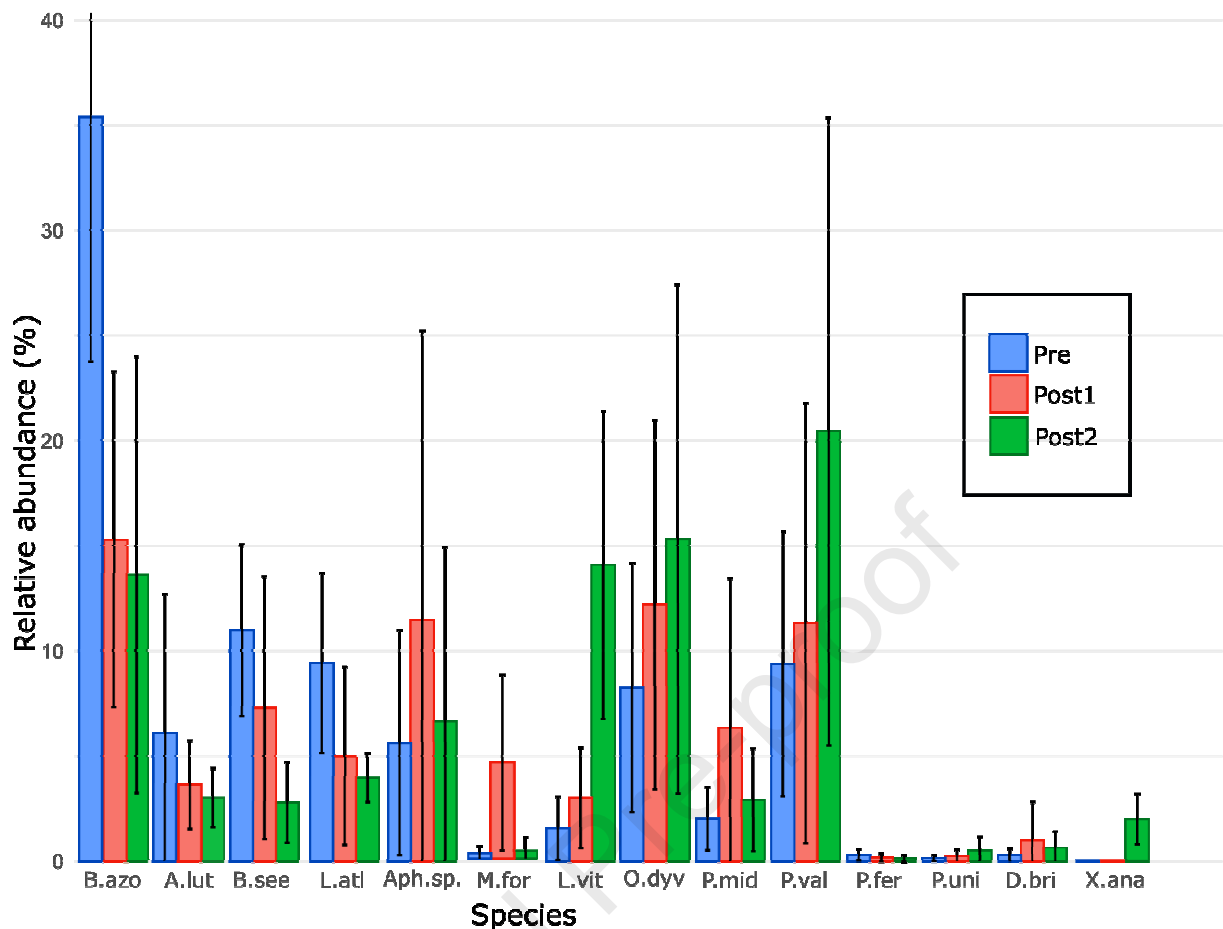


Figure 8. Mean and standard deviations of densities for the most abundant species among the experimental quadrats on the active Montségur edifice before the disturbance (Pre) and one/two years after the disturbance (Post1 and Post2). Species acronyms: B.azo – *Bathymodiolus azoricus*; A.lut – *Amphisamytha lutzi*; B.see – *Branchipolynoe seepensis*; L.atl – *Lepetodrilus atlanticus*; Aph.sp. – *Aphotopontius sp.*; M.for – *Mirocaris fortunata*; L.vit – *Lurifax vitreus*; O.dyv – *Oncholaimus dyvae*; P.mid – *Pseudorimula midatlantica*; P.val – *Protolira valvatoides*; P.uni – *Prionospio unilamellata*; D.bri – *Divia briandi*; X.ana – *Xylodiscula analoga*.

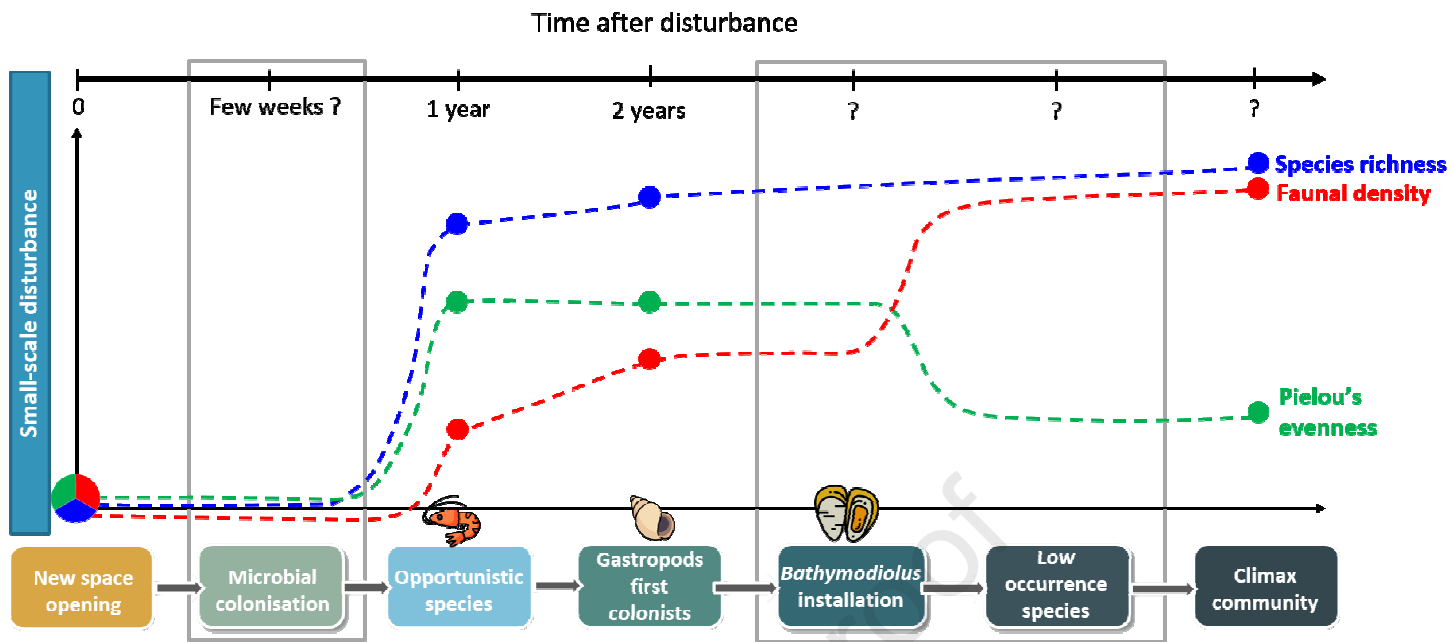


Figure 9. Conceptual model of colonisation and ecological succession until climax after a small-scale disturbance on the Lucky Strike vent assemblages (MAR). Evolution of species richness, faunal densities and Pielou's evenness index during the recovery process, based on the main results of our disturbance experiment (solid dots) and inferred from the literature (grey boxes).

Highlights

- Novel experimental approach by inducing small-scale disturbance to assess the recovery of vent communities.
- Full recovery of faunal taxonomic richness within 2 years after the disturbance
- Incomplete recovery of faunal densities and enhancement of species evenness in post-disturbance communities
- Gastropod species appears to be the pioneer colonists of active vent assemblages
- There are differences in the recovery rate of active vent in comparison to peripheral area and inactive structure.

Declaration of interest

The authors declare no competing interests.

Journal Pre-proof